Chapter 6

Application of Conducting Polymers

The study of CPs is a challenging exercise from both a fundamental point of view and the commercial potential these materials have. Many of the applications are based on the fundamental principles of physics and we concentrate on these issues in sections 6.1 – 6.6. In the applications arena, CPs are bringing radical innovations such as in electromagnetic interference shielding[1], CPs as pixel drivers in displays and electronic alfactometer (nose)[2]; completely new applications such as in electrochemical drug delivery[3] and novel applications such as artificial muscles[4] and bioaffinity sensors[2]. CPs have the potential of creating their own market segment as has been proved in the case of plastic batteries and organic light emitting devices in large screen displays[5]. Taking these factors into consideration, it is a plausible technological strategy for any industry that feels its technology would be threatened in the near future and/or wishes to be first on the market with an innovation to embark on researching CPs. As mentioned earlier, there is ample evidence indicating immense worldwide interest in CPs and astonishing applications successes thus far.

The combination of metal-like or semiconducting conductivity and processibility of classical polymers has created opportunities for a large range of applications for CPs[6]. The unique properties of inherently CPs stem from:

(i) the possibility of fine-tuning the conductivity by adjusting the amount of dopant incorporated within the polymer
(ii) doping/dedoping reversibility
(iii) the optical absorption characteristics in the ultraviolet, visible and near infrared spectra, as well as its electromagnetic absorption characteristics[6,7]. Some of the advantages of CP based devices compared to inorganic materials for the same functions include low weight, cost, flexibility and ability to form large surface areas as compared to conventional semiconductor materials[7].

Several polymers have been tested and proven to work in a variety of applications. Figure 6.1 illustrates some of the applications of Pan[6]. Despite the relatively poor success in providing a satisfactory explanation of the charge transfer mechanism in CPs, a number of products have achieved commercial success. In most instances the success has been attributed to consistent and reproducible responses of CP material to different stimuli. Individuals, companies and universities currently own several patents on the synthesis and device fabrication of these materials. Some of the commercialized products based on Pan are:

- Antistatic layers in computer disks by Hitachi Maxwell [2].
- Camouflage by Milliken and Co[2].
- Dispersible Pan powder version - jointly developed by Allied Signal, Americhem and Zipping Kessler[2].
- Electrostat loudspeaker - 0.1 μA Pan on 6 μm polyester film.
- Incoblend electrostatic dissipation. This technology is being utilized as an antistatic component for computers[1].
- 3V - coin-shaped batteries by Bridgestone-Seiko[2].

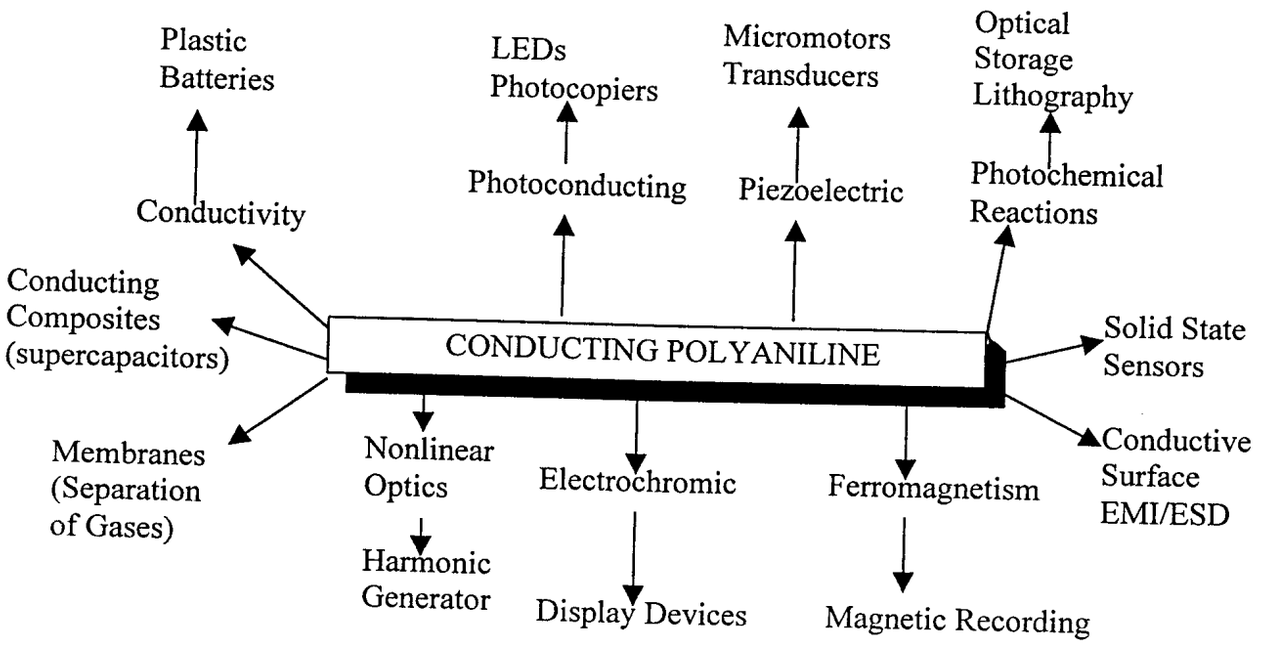

Fig (6.1): Applications of Pan[6].

6.1 Photoelectric conversion

CPs can be used in place of inorganic materials to convert solar irradiation into electric signals. Advantages of using CPs over inorganic materials include: ease of fabrication, lower cost of fabrication and environmentally friendly disposability. Grandstrom *et al*[8] obtained open-circuit voltages greater than 2 V, whereas *p*-type silicon based solar devices produce less than 1 V. This result implies that, compared to silicon, fewer polymer-based devices need to be cascaded to obtain the same net output voltage[8].

A bandgap exists between the (HOMO) and (LUMO) molecular orbitals. The bandgaps of most photovoltaic polymers lie in the range 1.5 – 3 eV, and as such are comparable to the energies of photons whose frequencies lie within (or just outside) the visible spectrum. This makes the polymers ideally suited for fabricating optoelectric devices. An incident photon has sufficient energy to excite an electron from the HOMO into the LUMO band of the polymer. This event creates an electron coupled to a hole – the exciton, and their motion through the material remains coupled. Figure 6.2 illustrates an **exciton** in a polymer[8].

The bound electron and hole are split at the electrode/polymer interface, as illustrated in figure 6.3. The electrons are collected at the lower work function electrode and holes at the higher work function electrode. The voltage output depends on the work function difference between these two electrodes.

In general there are two principles for photoelectric conversion[5]

(a) Utilize junctions of semiconductors such as *pn* junction or Schottky contact.
(b) Photochemical processes which produce electrical output from a photochemical reaction.

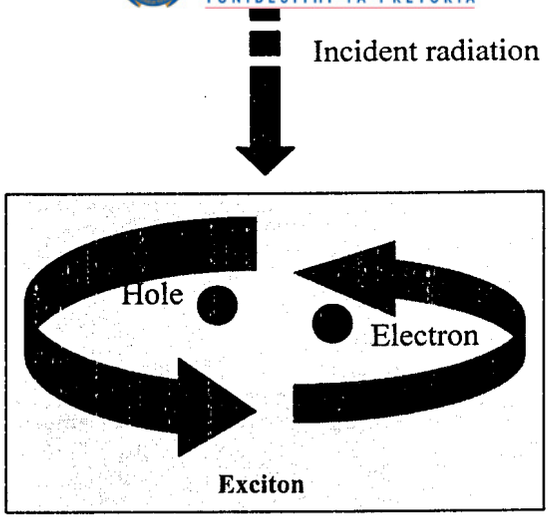

Figure (6.2): Excitons are produced in a CP. An incident photon produces bound electron-hole pairs called excitons, which transport charge in photovoltaic polymers[8].

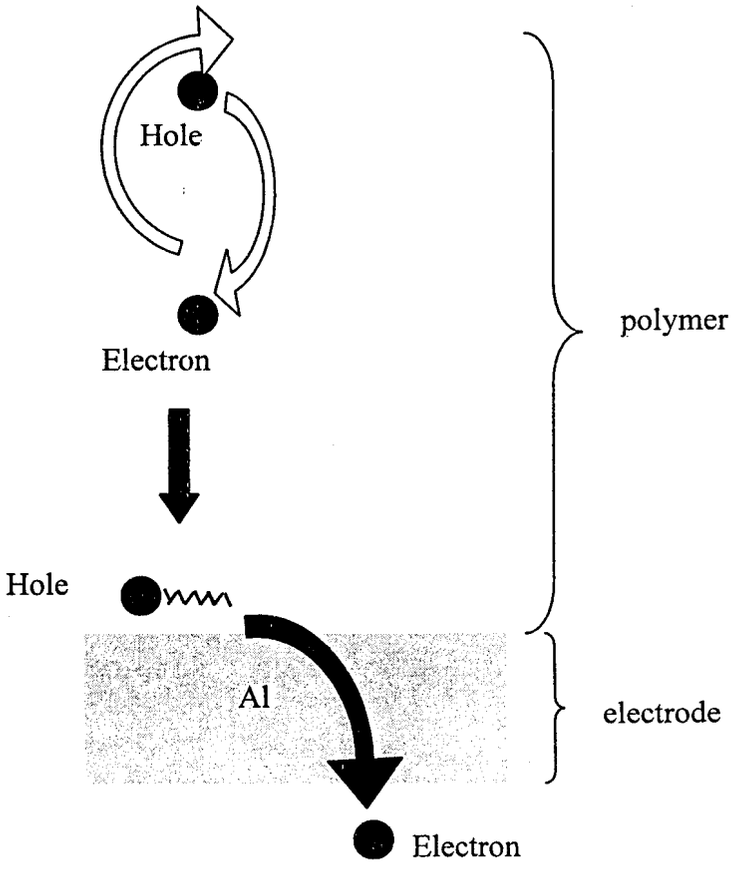

Fig (6.3): Excitons dissociate at the interface between materials having different ionization energies and electron affinities[8].

6.1.1 Design principle

The lifetime of excitons is short and only excitons that are formed within ~10 nm of the junction will ever reach it. Hence, when considering the mobility range of charge carriers in CPs (10^{-7} to 0.5 $cm^2V^{-1}s^{-1}$) their lifetime is in the region of picoseconds[8]. By creating interfaces among CP molecules of differing electron affinities, it is possible to enhance the probability of electron transfer between molecules. Interpenetrating networks of electron-accepting and electron-donating polymers can be used in the place of polymer/metal heterojunctions. Research into polymeric photovoltaics is at an early stage and we shall briefly describe such a device formed using a metal/polymer/metal structure, as depicted in figure 6.4[9].

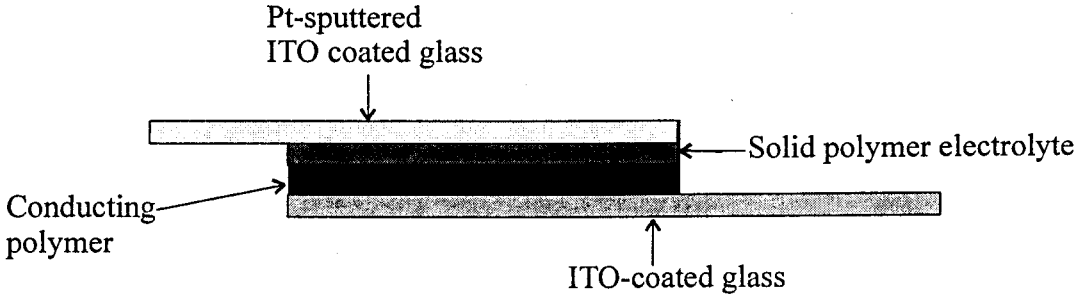

Fig (6.4): Construction of a photovoltaic device[9].

Although the photoelectric conversion of these devices is not high (2 % for polythiophene in sunlight), they can be used as sensors and for photoelectric devices. Recent advances in the efficiency of solar cells, based on organic dyes, encourages the development of devices with high performance at low cost[1]. The problem with durability could be overcome in the future by both fundamental and application-directed research. The variety of polymeric and organic materials should promise to open a new era of photoelectric conversion devices[8].

6.2 Organic light emitting devices (OLED)

OLED emit light as a result of the radiative recombination of electrons and holes electrically injected into the luminous polymer, which is sandwiched between two electrodes on a transparent glass. Typical OLED are constructed by sandwiching a

layer of luminescent CP between an anode (usually Indium Tin Oxide (ITO), because of its high work function) and a cathode (metals such as calcium, aluminum or magnesium/silver alloy with work functions 2.9, 4.3 and 3.7 eV respectively) on top of a glass substrate[10]. Figure 6.5, depicts a simple design of an OLED with poly (p-phenylene vinylene) (PPV) as the electrochromic CP.

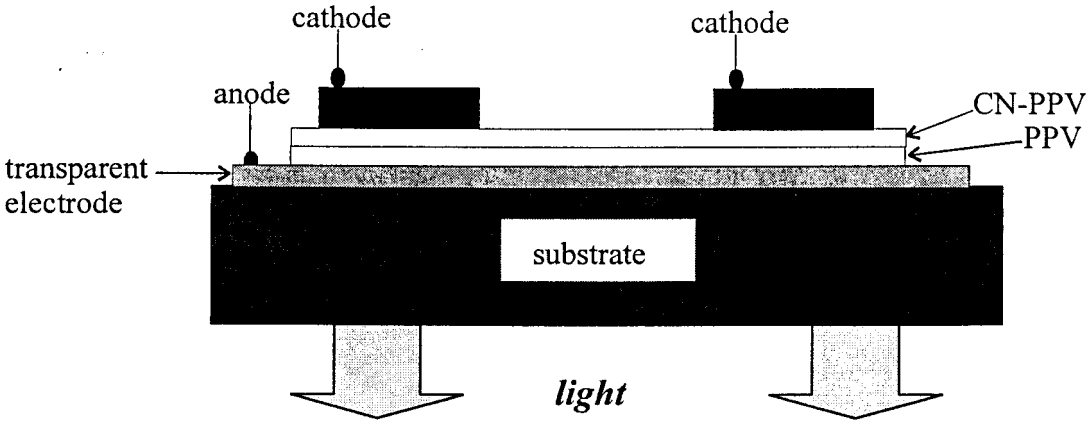

Fig (6.5): A light emitting device from CN-PPV[5]. CN-PPV stands for Poly(2,52',5'-tetrahexyloxy-8,7'-dicano-diphenylvinylene).

6.2.1 Operation

When an electric current is applied across the cathode and anode contacts, the potential developed between the electrodes ensures that electrons (negative charge carriers) flow into the polymer. Discharge of electrons by the anode results in holes being left in the polymer. Electron/hole recombination results in photon emission. The current-voltage curves of the device are diode characteristic[10]. At reverse bias conditions (ITO as the cathode and calcium as anode), charge injection is difficult and only leakage currents are measured. At forward bias, holes and electrons are injected into the polymer films from the ITO cathode and calcium anode, respectively. The energy level diagrams for such a device are shown in figure 6.6[5].

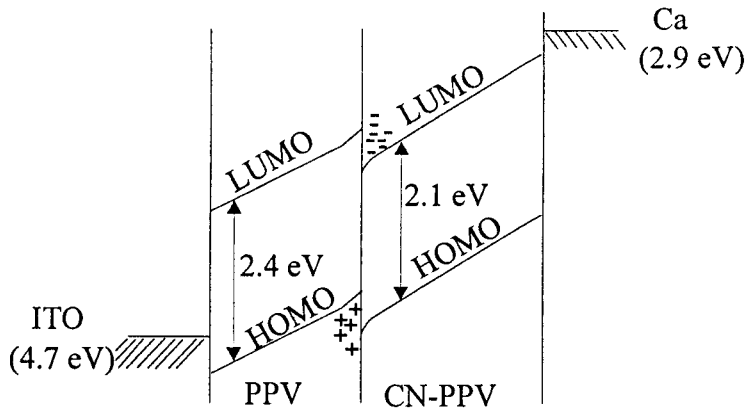

Fig (6.6): Energy level diagram for an OLED under forward bias[5].

The polymer/metal interface determines charge injection and therefore plays a crucial role in the operation of the devices. Due to a low dopant concentration the luminescent CPs are often treated as intrinsic semiconductors with a rigid band structure. The primary mode of electron injection in OLED is proposed to be field emission tunneling at high electric fields[5,10].

Applications of OLED include bright light for large area displays, alphanumeric displays and light emitting diodes[5, 10].

The advantages include: low cost, ease of fabrication, power efficiency, large surface area, bright, multi color display, mechanical flexibility and light weight[5].

6.3 Electrochromic windows

Electrochromic windows utilize the property that electroluminescent CPs such as Pan change color during electrochemical oxidation/reduction processes. For example, Pan changes color from pale yellow to green to violet and during reduction the color will change from violet to green and then to yellow[9]. By utilizing this property, the amount of light passing through a window of this material can be controlled.

Electrochromic windows are fabricated on thin semitransparent layers of conducting glass usually ITO. A schematic representation of an electrochromic window using a transparent solid polymer electrolyte is shown in figure 6.7.

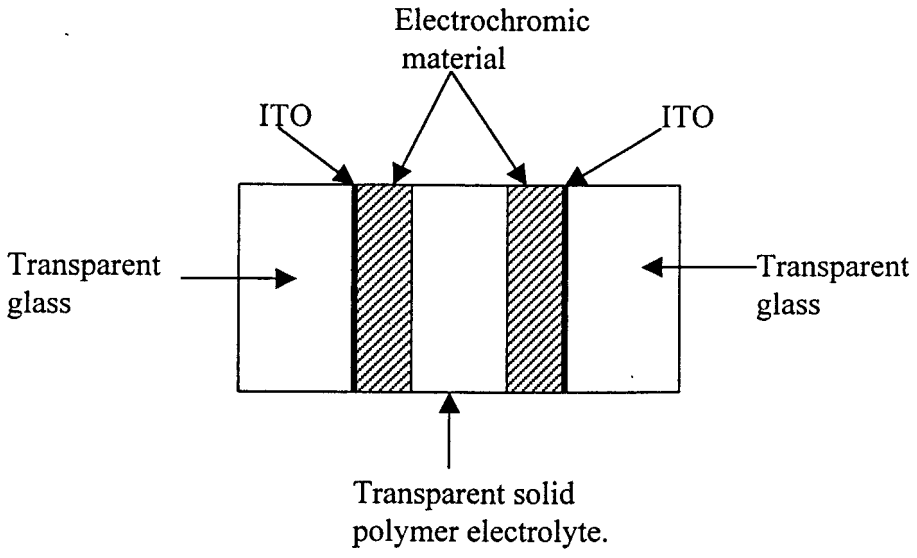

Fig (6.7): A schematic of an electrochromic window; Pan is used as the electrochromic material and polyethylene oxide containing $LiClO_4$ is used as the transparent solid polymer electrolyte[9].

Possible applications include: smart windows that are made opaque by simply applying a current, and the use by defense force industries[9].

6.4 Artificial muscles

Artificial muscles are devices made out of intrinsic CPs, which transform electrical energy into mechanical energy through electrochemical reactions occurring at the molecular level in the solid CP[4].

These electrochemomechanical actuators function by using electrochemically induced:

- changes in dimensions of the CP
- changes in relative dimensions of the polymer and a counter electrode or,
- changes in total volume of a CP electrode, electrolyte, and counter electrode[11].

When intrinsic CPs are used as electrodes in ionic media, they are oxidized and reduced in a reversible way. Linked to this electrochemical process, a reversible change in volume takes place[4]. Therefore, by applying a voltage to such a cell, its

volume can be changed in a defined manner[4]. Emerging applications include: devices for microrobotics, microvalves, microdevices and medical instrumentation (see figure 6.8: microtweezers).

6.4.1 Operation

An electric pulse, generated by electrochemical equipment, arrives via metal wires at the CP films, driving an electrochemical reaction. The device operates by the electrochemical transfer of dopant between the CP layers, separated by an adhesive ion-conducting layer[12]. The electrochemical reaction promotes a change in the volume of the film, giving a concomitant macroscopic movement of the bilayer and mechanical energy. The electrochemical reaction is linked to the conformational changes of the polymer chains together with a flow of ions and water through the polymer - solution interface[4].

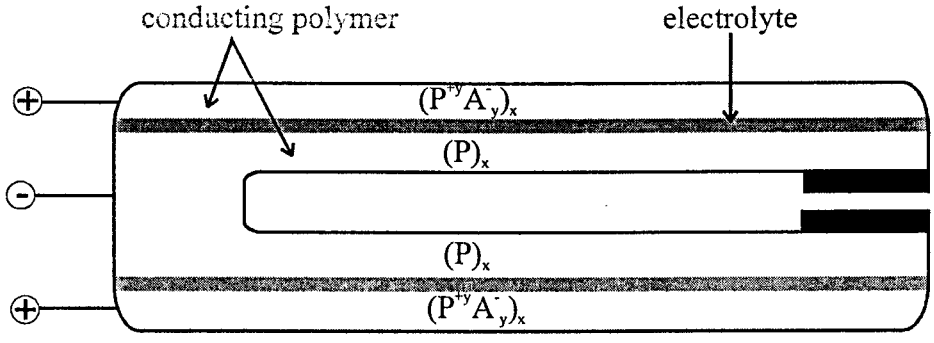

Fig (6.8): Paired bimorph actuators used as micromechanical tweezers. $(P)_x$ represents any CP, e.g. Pan and $(P^{+y}A^{-}_{y})_x$ represents a CP doped by an anion A^-. Electrochemical transfer of dopant from the outer layer to the inner layer as a result of reversing the electrode potentials of each bimorph causes the opening of the tweezers[4,12].

Advantages of these actuators include: low voltage needed for operation (1V) compared to 100V for electrostatic tweezers and high mechanical advantage as compared with piezoelectric polymers. The disadvantages include limitation on cycle time (2.56 seconds were required to reach a 90^0 turn) for the device[12].

6.5 Humidity sensors

Recently, the demand for humidity control has increased in fields such as air conditioning systems, electronics manufacturing and drying processing for ceramics and foods[11]. However, commercial humidity sensors are far from satisfactory since a linear response is valid for only a limited humidity range and hysteresis is often involved in the measurement of the response and humidity curves[11].

A humidity sensitive film has been synthesized consisting of soluble Pan 0.28% volume and 99.72% polyvinylene alcohol (PVA). The conductivity of Pan – PVA composite was proportional to the relative humidity, and the linearity was valid from 3×10^{-5} to 1.5×10^{-1} S/cm. The conductivity of the composite film varied depending on the doping level of Pan, which was dependent on the concentration of water molecules around the conducting polymer[11]. The conductivity versus humidity curves for Pan-PVA composites are shown in figure 6.9.

The excellent linear dependency of conductivity on humidity, reflecting the reversible incorporation and ejection of water molecules occurring in the composite film, is favorable for the construction of a humidity sensor[11].

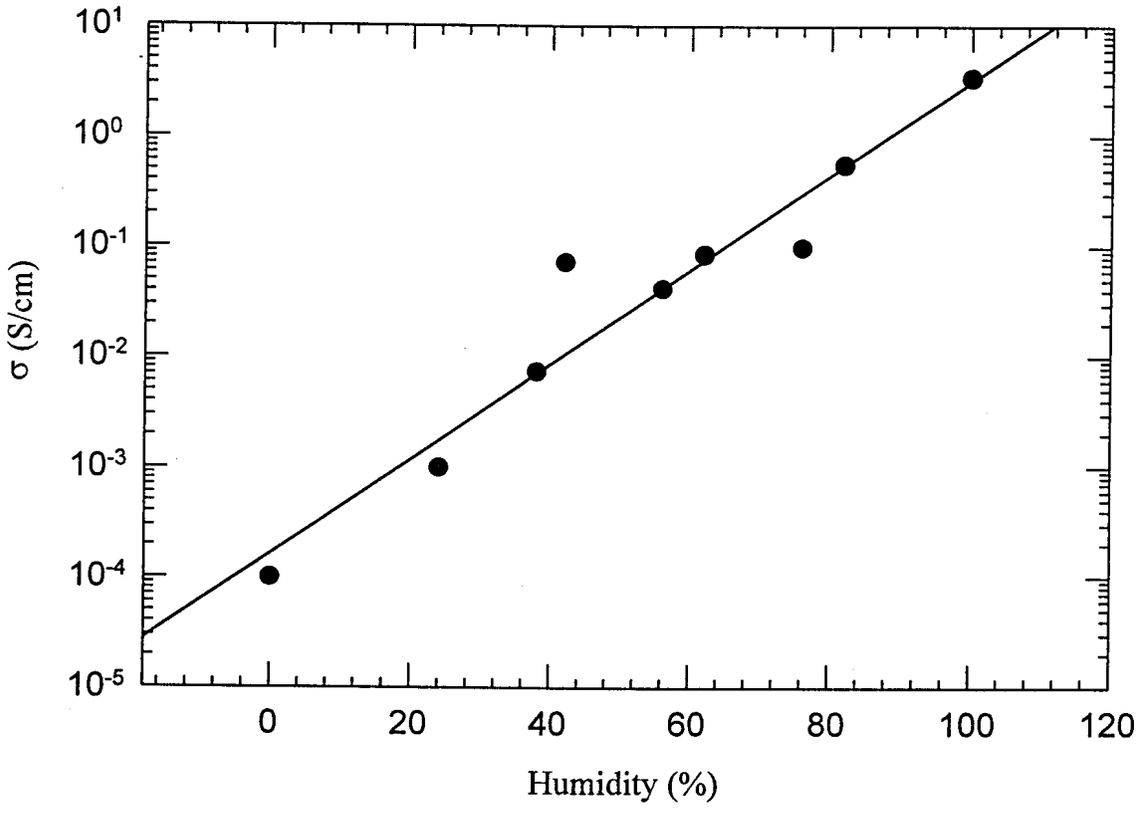

Fig (6.9) A schematic illustration of the relationship between humidity and temperature of a Pan–PVA composite film[11].

6.6 Corrosion prevention

The use of CPs as anti-corrosion coatings addresses the following issues, which the traditional methods (coating the metal with a material, chemical "conversion coatings" and cathodic protection) do not:

- Environmental issues, such as the unacceptability of chromates (used in conversion coating).
- Ease of application and practicality, e.g. contrary to cathodic protection.
- Cracks and pinholes, as well as slow corrodant diffusion to the metal surface. This problem is rampant in the conventional coating.

A CP, such as Pan, can be used to coat metal surfaces in order to prevent corrosion. Various methods are used for coating, including painting with the polymer, spraying and dipping the metal in liquid polymer. The use of a CP coating on a metal creates a built-in electric field, resulting from the interfacial, positive dipole space charge

layers[5]. This creates a force (F = -eE, figure 6.10), that opposes electron transfer from the metal to oxidizing species in the external environment (such as oxygen). A bending of the CP bands occurs at the metal/CP interface (figure 6.11)[5]. An important and distinctive feature of this method is that the electric field created is intrinsic and extends up to 250 μm in dimension (the field extends across small pinholes and cracks) providing protection[5]

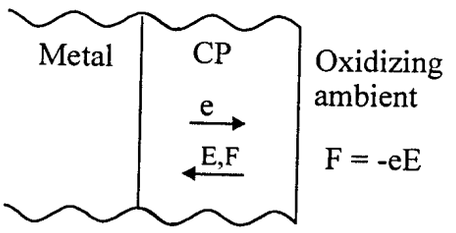

Fig (6.10): The metal/CP interface, showing the intrinsic electronic barrier to corrosion generated by the coating of CP[5].

Promising applications are in the industrial cooling-water treatment plants where phosphates and heavy metal salts traditionally used raise environmental pollution concerns[3, 5].

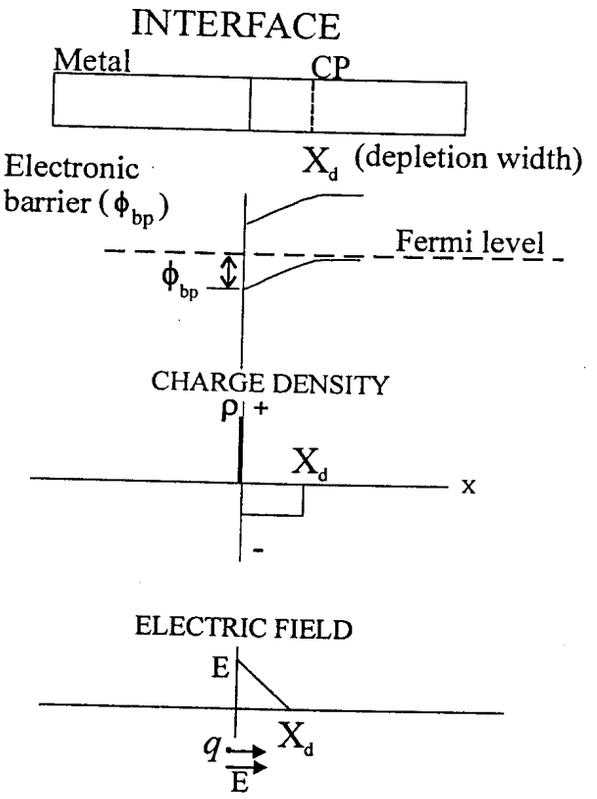

Fig (6.11): The metal/CP interface, showing band bending and development of interfacial space charge and electronic barrier to corrosion[5].

Reference:

1. J. Joo, A. J. Epstein, App. Phys. Lett. **65**, 2278 (1994).
2. O. A. Sadik, Electroanalysis **11** Number 2, 839 (1998).
3. A. J. Epstein, MRS Bulletin **22**, 16 (1997).
4. T. F. Otero, Handbook of Organic Conductive Molecules and Polymers **4** (Ed. H. S Nalwa), John Wiley and sons: New York (1997).
5. Conducting Polymer Fundamentals and Applications, (Ed. P. Chandrasekhar), Kluwer academic publishers: Boston (1999).
6. D. C. Trivedi, Handbook of Organic Conductive Molecules and Polymers **2** (Ed. H. S Nalwa), John Wiley and sons: New York (1997).
7. K. Gurunathan, R. Marimuthu, D. P. Amalneker, Mat. Chem and Phys. **61**, 173 (1999).
8. http://pubs.acs.org/hotartcl/ci/oo/apr/065wallace.html
9. E. Kim, S. B. Rhee, Electrochem. Soc. **144**, number 1, 227 (1997).
10. Masao Kaneko; Handbook of Organic Molecules and Polymers **4** (Ed. H. S Nalwa), John Wiley and sons: New York (1997).
11. F. Krok, Mat. Sc. Forum **122**,150, Ed. J. Przyluski & S. Roth, (1993).
12. R.H. Baughman, L.W. Shacklette, Science and Application of Conducting Polymers, 52, (Ed.: W R Salaneck), Bristol: England (1991).

Chapter 7

Experimental Techniques

In order to determine charge transfer phenomena in CPs, direct current (DC) current-voltage measurements were done on Pan films and pellets at temperatures above 300 K and at low temperatures down to 30 K. Fourier transform infrared spectroscopy (FTIR) and thermal analysis methods were applied to determine the effect of annealing on the polymer. The following types of Pan were used in the present work:

- Electrosynthesised Pan (HCl doped).
- Chemically synthesized Pan (HCl doped).
- Commercial Pan (Aldrich).

Chemically synthesized and commercial Pan were available in both the doped and undoped form. The undoped form was dissolved in N-methyl-2-pyrrolidinone (NMP) and spun to form thin films. Doped forms were pressed to form pellets and used in FTIR, thermal analysis and annealing experiments. The experimental work described in this chapter covers all the steps in electrochemical and chemical synthesis. This chapter comprises two sections,

(i) *Experimental procedures, covering polymer synthesis and*
(ii) *Experimental techniques, covering the experimental set-ups and measurements*

The flow chart, figure 7.1, summarizes the processes from polymer synthesis, sample preparation to material characterization in this work. The synthesized Pan is in its doped state, which is insoluble in most common solvents besides strong acids. To process Pan into thin films, we dedoped the chemically synthesized Pan before dissolving it in an organic solvent (NMP).

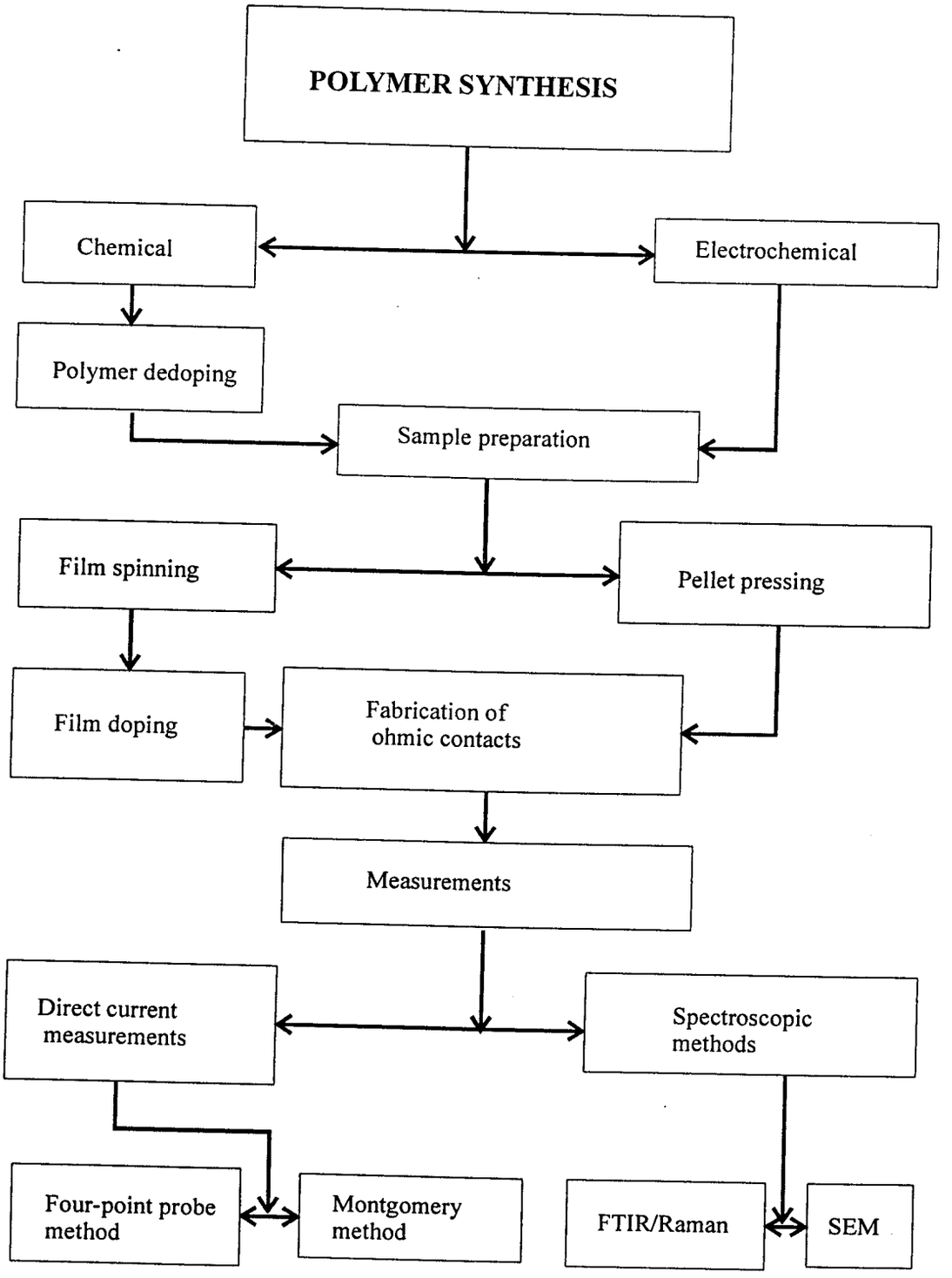

Fig (7.1): A schematic layout of the procedures used in the present work

7.1 Chemical synthesis of polyaniline

Chemical synthesis was the preferred method to obtain high quantities of the polymer. Through applying the method described below, we were able to obtain a Pan emeraldine yield of approximately 14 g. An oxidant, ammonium persulphate $(NH_4)_2S_2O_8$, was used to effect chemical polymerization of aniline under acidic conditions, pH 1-3[1]. The function of the oxidant was to withdraw a proton from an aniline molecule, without forming a strong coordination bond with either substrate/intermediate or with the final product. The selected pH conditions favored the formation of Pan, which was not suitable for the formation of strong metal chelates [1].

7.1.1 Requirements

i. 50.005 g $(NH_4)_2S_2O_8$
ii. 20.002 g aniline
iii. 750 ml 1.0M HCl
iv. excess 3 wt % NH_4OH
v. 20 liters distilled H_2O

7.1.2 Procedure

50 g of $(NH_4)_2S_2O_8$ was dissolved in 500 ml of ice-cold 1M HCl. This was added to a stirred solution of 20 g aniline in 250 ml ice-cold 1M HCl[2]. An ammonium persulphate solution was added over a time of abut 30 minutes. Stirring of the solution was continued for 2 hours after which the mixture was suction filtered using a Buchner funnel and washed with distilled water until the filtrate was colorless[2]. During washing the water level was always above the polymer coke to prevent drying which might cause uneven washing. Pan (ES) was obtained as a dark green precipitate.

7.1.3 Preparation of emeraldine base

The freshly prepared precipitate – ES was deprotonated by stirring in excess 3 wt% ammonium hydroxide solution. The deprotonated precipitate was washed in distilled water until the filtrate (EB) was colorless. To remove excess oligomeric impurities we washed the precipitate in 500 ml of acetone [2].

7.2 Glass substrate preparation

Polymer films were formed on glass substrates, which had to be cleaned initially to improve the contact between the glass and the polymer. Wax used for fixing the glass on a silicon wafer before dicing was removed by firstly heating the wafer and the glass until the wax softened. The glass was put in boiling acetone for 15 minutes and then rinsed in distilled water before immersing it in boiling propanol for 10 minutes. Finally the glass was rinsed in distilled water and blow dried with nitrogen gas.

7.3 Polymer spinning

A film of Pan was produced through spinning a drop of the polymer solution onto a glass substrate[3]. The Pan solution was prepared through dissolving Pan EB in NMP [3] until the solution saturates. It was then centrifuged for two hours at 4000 rpm to separate lumps of the undissolved polymer. This solution was then spun onto a square glass substrate at 1000 rpm [3] for a minute.

Two methods were used for film drying, drying in an oven under a fan at a temperature of 40°C and drying in a natural environment at room temperature for 48 hours. An average film thickness of 50 μm was obtained. Pan films were used for conductivity measurements over the temperature range ($30 \leq T\,(K) \leq 300$).

7.3.1 The EC101D photoresist spinner (*instrumentation*)

The major components of the photoresist spinner are as listed below:

i. Motor controller: consists of a tachometer for controlling the speed of the spinner, a cycle timer for controlling the spin cycle and a motor speed controller that works together with the tachometer.

ii. A vacuum pump: for fixing the substrate in position.

7.4 Film doping

A thin film of EB was exposed to vapors of HCl for 1 minute. The film was doped by the vapor to green ES from purple EB. Uniform doping was ensured, through exposing both sides of the film to the HCl vapors.

7.5 The depth profiler

An Alpha-Step 200-depth profiler measured the thickness of soft Pan films spun onto glass slides. Thickness was analyzed as the difference in the height between the virtual zero level and the surface of the film. Figure 7.2 illustrates the movement of a stylus in measuring thickness.

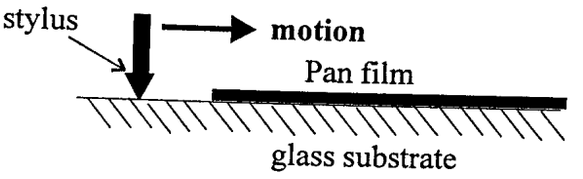

Figure (7.2): Stylus motion during thickness measurement

The Alpha-Step 200 samples up to 2000 data points on each scan, providing up to one sample every 400Å. It can identify discontinuities in the film in tens of Angstroms and can measure surface profiles below 200Å and up to 160 microns.

7.6 Electrochemical synthesis of polyaniline (Pan)

The anodic oxidative polymerization of aniline is the preferred method to obtain a clean and thin coherent film of Pan [1,4]. Electrochemical synthesis was achieved by sweeping the potential between two potential limits – 0.2 to 0.8 V versus silver in silver chloride (Ag /AgCl) counter electrode at a scanning rate of 50 mV/s [1, 5, 6, 7]. The electrolyte was a solution of 0.2M aniline in 1.0M HCl with a pH of about 1. Dark green Pan (ES) was deposited onto the anode [7].

After removing electrodeposited Pan (ES) from the platinum electrode by stripping it off with a blade, the electrodes were cleaned of excess polymer by immersing them in nitric acid until the polymer disappeared. Then a process involving rinsing the electrodes in distilled water, boiling in acetone for about 5 minutes followed by immersing them in boiling propanol was applied. Finally, the electrodes were rinsed in distilled water.

7.6.1 Instrumentation

The electrochemical cell is constructed from a vessel containing a solution of a monomer (aniline) together with an acid (HCl) [4]. Electrochemical polymerization was carried out using an EG & G Model 362 scanning potentiostat. A three-electrode cell was employed with platinum foils (2 cm x 2 cm) used as both counter and working electrodes. Silver in silver chloride was the reference electrode. Pan ES deposits on the working electrode were stripped off and filtered in distilled water. Alternative cell configurations used in this work included graphite as working electrode versus platinum counter electrode, indium tin oxide as both working and counter electrodes, platinum coated glass was also used as both working and counter electrodes.

7.6.2 Problems encountered during synthesis

i. Electrochemical deposition using indium tin oxide (ITO) coated glass as working electrode and graphite rod as counter electrode produced a very small yield. It was later discovered that ITO was dissolving in the solution. We therefore decided to use platinum-coated glass instead of ITO.

ii. Using platinum coated glass also resulted in problems because platinum was easily removed by the crocodile clamp grips used to suspend the glass in the solution. Considering the cost of platinum and the deposition process, it was found economically necessary to find an alternative source of working electrode. We obtained platinum foils measuring 1.5 cm x 1.5 cm and a thickness 0.07cm.

iii. Using graphite as working electrode, Pan deposits were too loosely bound onto the electrode plate such that by withdrawing the electrode from solution, all the deposit was lost into the solution.

iv. Accumulation of air bubbles on the working electrode, which were insulating, stopped the deposition process. A suitable current of 10 mA was chosen for the potentiostat.

7.7 Deposition of metal contacts

A resistive evaporation system was used to deposit metals onto the glass substrates for the making of platinum and gold electrodes. An attempt was also made to form ohmic metal contacts on the polymer films using this method. The first and most important step was the cleaning of the glass substrates. Glass substrates were boiled in aqua regia (a mixture of hydrochloric acid and nitric acid in the ratio 3:1) for 10 minutes. The glass was then rinsed in distilled water and then boiled in trichloroethlyene (TCE) for 3 minutes. From TCE, the glass was put into boiling iso-propanol for 3 minutes, rinsed in distilled water and dried with nitrogen gas.

Deposition of thin ohmic gold films onto a glass substrate and a doped Pan surface was accomplished by use of an evaporation system. The main components of the deposition

system include a bell jar, a substrate holder, a thickness monitor, a shutter, a source, a lower shield/reflector, a transformer and a vacuum pump[8].

The gold was placed into the source and a vacuum of about 10^{-5} Torr (7 mbars) was attained before evaporation could start. The Joule heat created by the current passing through the source resulted in evaporation of the gold. The temperature was controlled through slowly increasing the current. A deposition rate of 4 Å/second was maintained through adjusting the current output. The maximum temperature on the Pan sample was maintained below 40°C.

For making platinum electrodes, platinum was deposited onto a titanium coated glass surface to a thickness of about 2000 Å. The titanium/glass substrate was first annealed at 250 °C in an argon environment to improve the adhesion between the glass and metal contact.

7.8 Electrical measurement techniques

Two methods (the four-point probe and Montgomery) were applied in the measurement of the electrical properties of Pan. In applying the Montgomery method, graphite paste was used to attach copper wires at the four corners of the sample (figure 5.2 chapter 5).

7.8.1 Fabrication of Ohmic contacts

Pan ES (Aldrich, electrosynthesised and one synthesized in our laboratory) were pressed to form pellets of thickness between 0.02 and 0.5 mm at pressures between 8 and 20 tons. The resistive evaporation technique (as explained in the previous section) was used to make ohmic contacts by the deposition of gold onto the surface of the materials through a mask to create contacts with a diameter 0.75 mm. For the Montgomery method, graphite paste was used for making the ohmic contacts, between the connecting wires and the sample surface.

7.8.2 The four-point probe method

The four-point probe method was used in the measurements of the I-V properties of Pan in pellet form, see figure 5.1, chapter 5.

A small current was passed through the outer two probes and the voltage was measured between the inner two probes [9, 10]. The current source was a model HP 3245A and the voltage source was model HP 3457A with an internal impedance of 10 GΩ. The conductivity is defined by Ohm's law, as the ratio of the current (I) flowing through the sample and the electric field (E) [9, 10]. For all pellets with dimensions W << d and d >> s, the conductivity, σ, was calculated as:

$$\sigma = I/u2\pi s \qquad [7.1]$$

Where, I is the measured current, u is the applied potential difference and s is the pellet thickness.

7.8.3 Montgomery method

In the Montgomery method, electrodes were attached at the four corners of a square polymer sample, (figure 5.2, chapter 5) [10, 11]. Current was applied on electrodes *1* and *2*, while electrodes *3* and *4* measured voltage. From the current-voltage measurements, resistivity was calculated[11]. For thin samples resistivity is expressed as:

$$\rho = Hl_3R \qquad [7.2]$$

where H is a function of l_2/l_1. The value of H used in the result analysis was 4.531, since l_1 was made equal to l_2[11]. R is the ratio (V/I) of the voltage between the two contacts and the current. After mounting the sample on the sample holder, the temperature was lowered to 30 K. Thereafter, the temperature was increased in intervals of 10 K from 30

to 380 K. For each temperature interval a set of current and voltage measurements were taken. Low temperatures were achieved using a cryostat.

7.9 Temperature controller for heating pellets

A power supply and controller supplied a voltage to an element over which a pellet of Pan rested. A feedback loop of the thermocouple was used to control the temperature and, using the temperature controller, it was able to adjust the rate at which temperature increased and the time taken between ramps. The voltage measurements were made using the four-point probe method.

7.9.1 Experimental setup

In order to anneal a pellet while monitoring the current-voltage behavior of the sample, a state of the art instrument was designed through interfacing, the four-point probe, a voltage source, a controller unit and a heating plate from "Linkman Scientific Instruments ltd." model TMS 93.

7.9.2 Operating modes

Experimental conditions were varied through use of the following operating modes of the system:

- The element was allowed to heat the pellet from room temperature to a maximum set temperature at rates typical of 20°C / min. A hold time of 10 minutes was deemed sufficient for the temperature of the pellet to homogenize. Current-voltage measurements were done within the 10^{th} minute.
- The heating element was able to heat the sample at different ramp rates. Different rates from 5 °C/min to 20 °C/min were used. The voltage was measured using the four-point probe technique.

- A current of 8×10^{-4} A was maintained on the pellet. Whilst the temperature rose at a rate of 5°C / minute, I-V measurements were taken.

7.10 Thermal analysis techniques

Thermal analysis is the measurement of changes in the physical properties of a substance as a function of temperature, whilst the substance is subjected to a controlled temperature variation[12]. Different samples and different conditions may alter the mass loss/temperature relationship and, for this reason, we used the simultaneous thermal analysis technique. This involved measuring the temperature and mass changes on the same portion of the polymer sample during a single temperature program[13]. Differential scanning calorimetry (DSC) and thermogravimetry analysis (TG) were performed simultaneously in this work.

7.10.1 Thermogravimetry (TG)

Thermal gravimetry was used in the detection of changes in the mass of the sample by reaction or evaporation. The mass of the sample is monitored against time or temperature while the temperature of the sample, in a specified atmosphere, is changed[12].
The apparatus comprises four main parts[12]:

- An electro-balance and its controller
- A furnace and temperature sensors
- A computer
- A data acquisition device[12].

Deviation of the balance beam from the null-position is measured using an electro-optical device with a shutter attached to the balance beam. The shutter partly blocks the light beam between the source and a photocell. Movement of the beam alters the light intensity on the photocell and the amplified output from the photocell is a measure of mass change[12].

7.11 Infrared spectroscopy

Fourier-transform infrared spectroscopy (FTIR) allows wavenumbers in the range 400-4000 cm^{-1}. Fourier transformation, is used to convert the measurement (interferogram) into a spectrum of the polymer. The region 400 to 4000 cm^{-1} is considered to be the mid-infrared region where vibrational and rotational bands are observed[14]. The effect of temperature and the period of heating on Pan salt and the base form were analyzed using FTIR spectroscopy.

7.11.1 FTIR Instrumentation

The optical system features a modular construction of the vacuum cabinet with infrared radiation focused on a beam splitter with an effective diameter of 10 mm. Interferograms were recorded at a vacuum of 100 mBar.

7.11.2 Sample preparation for FTIR

1000 mg of potassium bromide (KBr) kept at 100 °C in an oven was mixed with 50 mg of Pan. The mixture was finely ground in a pastel and mortar. A pellet was formed by pressing the KBr/Pan powder at a pressure of 8 tons[15].

References

1. D.C. Trivedi; Handbook of Conductive Molecules and Polymers **2**, 510, (Ed. H. S Nalwa), (Ed. H. S Nalwa), John Wiley and sons, New York (1990).

2. S. S Hardaker, X. Wang, R. V. Gregory, Pol. Prints **39**, 123 (1998).

3. Loon-Seng Tan, S. R. Simko, Pol. Prints **3**, 2 (1998).

4. A.G MacDiarmid, W. Zheng, MRS Bulletin **22**, 29 (1997).

5. Yen Wei, Yan Sun, Xu Tang, Poly Print **3**, 1 (1989).

6. M. Lapowski, Mat. Sc. Forum, **122**, 51 (1993).

7. V.C. Ngu Yen, K. Potje-Kanloth, Thin Solid Films **338**, 142 (1999).

8. E.B Graper, Handbook of Thin Films Processing Technology, A1.11: 1-A1.1: 2, (1996).

9. S. M. Sze, Physics of Semiconductor Devices, (Ed. S.M. Sze), New York (1981).

10. W. Pukacki, Mat. Sc. Forum **122**, 261 (1993).

11. H. C. Montgomery, J. App. Phys. **42**, 2971 (1971).

12 Thermal Methods of Analysis-Applications and Problems, (Ed. P.J. Haines), London: Chapman and Hall (1992).

13. Introduction to Thermal Analysis – Techniques and Applications, (Ed. M. E. Brown), New York: Chapman and Hall (1990).

14. S. Bandyopadhyay, J. App. Phys. **85**, 3671 (1999).

15. Practical Sampling Techniques for Infrared Analysis, (Ed PB Coleman), Boca Raton: CRS Press, (1993).

Chapter 8

Results

Experimental results aimed at determining the charge transfer characteristics of CPs are presented in this chapter. The present work uses methods ranging from simple four-point probe conductivity measurements to conductivity measurements using the Montgomery method in the temperature range 30 – 450 K. Charge transfer at low temperatures is important in the determination of whether conductivity is metallic, semiconducting or insulating and also for the one, two or three dimensionality of conductivity in the material. In the light of this, several models shall be tested for fitness to the observed conductivity. Conductivity determining factors such as moisture content of the material, temperature, homogeneity of the material, geometrical forms of the sample, synthesis conditions and pressure used in the pressing of pellets are dealt with. These conductivity-determining factors are crucial and need to be mentioned when stating a sample's conductivity.

We used four types of Pan, commercial Pan (doped by camphor sulfonic acid (CSA)), electrochemically synthesized (doped by HCl), commercial Pan (doped by HCl) and chemically synthesized Pan (doped by HCl). Due to the low yield of electrosynthesized Pan, our work was based on the commercial forms of Pan and the chemically synthesized Pan.

8.1 Determining the mode of charge transfer

Measurements were made to ensure that no significant contribution to conductivity was occurring due to ionic conduction (drift of negatively and positively charged ions), by passing a constant current through a Pan pellet and monitoring the potential difference as a function of time using the four point probe method. As table 8.1 shows, there is no significant change in voltage with time for a constant applied current. We conclude from

these preliminary and important results underlying this work that conduction in Pan is predominantly electronic and that contribution to charge transfer from ionic mechanism are not of significance. In the event of ionic conduction, the potential difference would increase as the ions get depleted.

Table 8.1: Variation of voltage with a constant current of 2 x 10^{-5} A

Time (min)	*Voltage (mV) ± 0.01*
0	0.084
1	0.084
16	0.084
70	0.085
4320	0.085

8.2 Conductivity of Pan pellets at room temperatures

Pan powder (chemically synthesized and HCl doped) was compressed at 7.4 x 10^7 Pa to form pellets with an approximate diameter of 12 mm and a thickness of 0.22 cm. Figure 8.1 illustrates room temperature voltage/current characteristics of three pellets pressed from the same batch of powder. The procedures discussed in section 7.5 were used in acquiring these results. This figure indicates that the conductivity of Pan is ohmic at room temperature.

It must be noted that for pellet samples no congruent relationship exists between conductivity and thickness (table 8.2). However as table 8.3 shows for Pan film samples at room temperature, conductivity increase with film thickness[1].

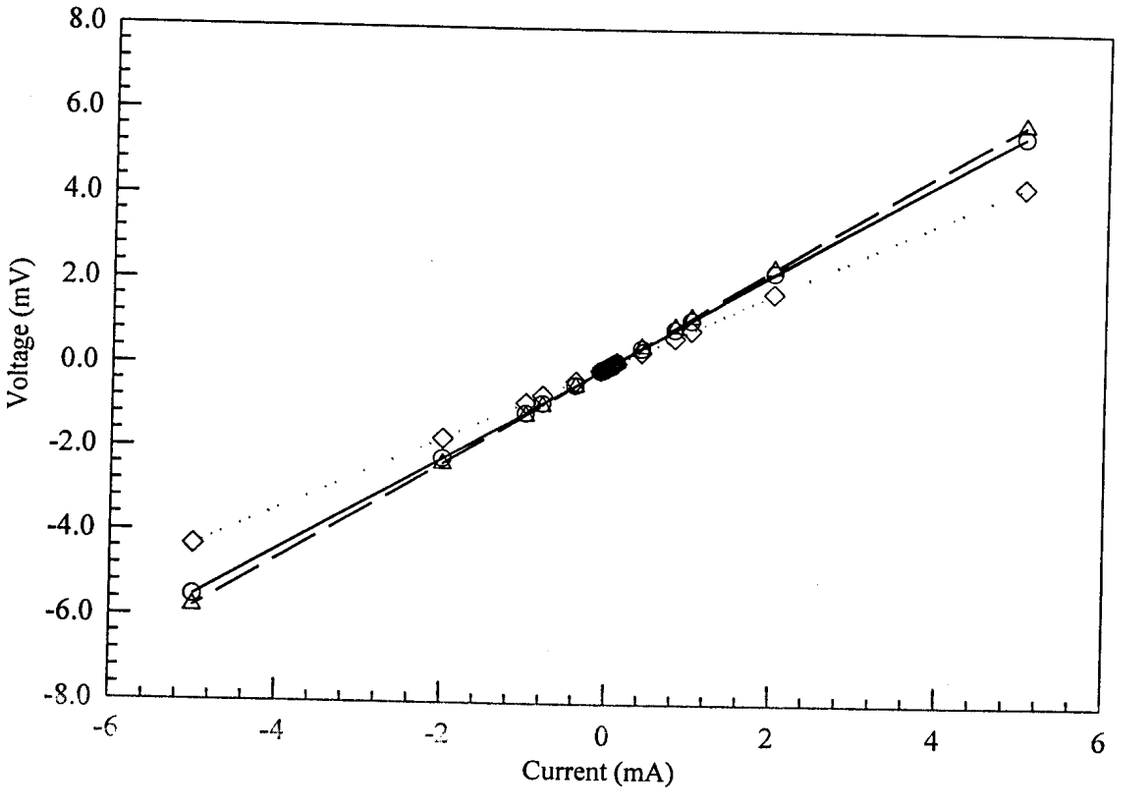

Fig (8.1): Room temperature current-voltage characteristics for three 0.022 cm thick Pan pellets pressed at 7.4 x 10^7 Pa.

Table 8.2: Conductivity of several pellets at room temperatures.

Sample	*Thickness (cm) ± 0.001*	*σ (S/cm) ± 0.2*
1	0.022	12.9
2	0.022	11.1
3	0.022	10.0
4	0.04	6.64
5	0.041	5.9
6	0.051	8.43
7	0.046	5.54
8	0.100	5.96
9	0.178	3.19
10	0.211	2.81

Table 8.3: Film thickness/conductivity relationship

Thickness ($\times 10^{-3}$) cm	*σ(S/cm)*
50	1×10^{-10}
100	1×10^{-7}
200	1×10^{-4}
300	1×10^{-4}
400	0.01
500	0.1

8.3 The effect of the temperature range, (30 < T (K) < 300), on the current-voltage properties of chemically synthesized Pan

It has been shown that temperature has an effect on the current/voltage characteristics of Pan[1,2]. The behavior of Pan has been determined as temperature varies from 30 K to 300 K using the Montgomery method. Currents up to 1 mA were applied over the temperature regime.

The spectra displayed in figures 8.2 ([A] and [B]) and figures 8.3 ([C] and [D]) illustrate the change in the current-voltage characteristics as the temperature increases from 30 K (figure 8.2 [A]) to 280 K (figure 8.3 [D]). As shown, the current-voltage characteristics of the material attain a direct relationship as temperature approaches 300 K (that is current/voltage spectra will be a straight line) for the particular fixed current range. The use of current values above 1 mA during the current-voltage measurements results in a heating effect due to the low conductivity of the polymer, thus measurements were restricted to reasonably low applied currents.

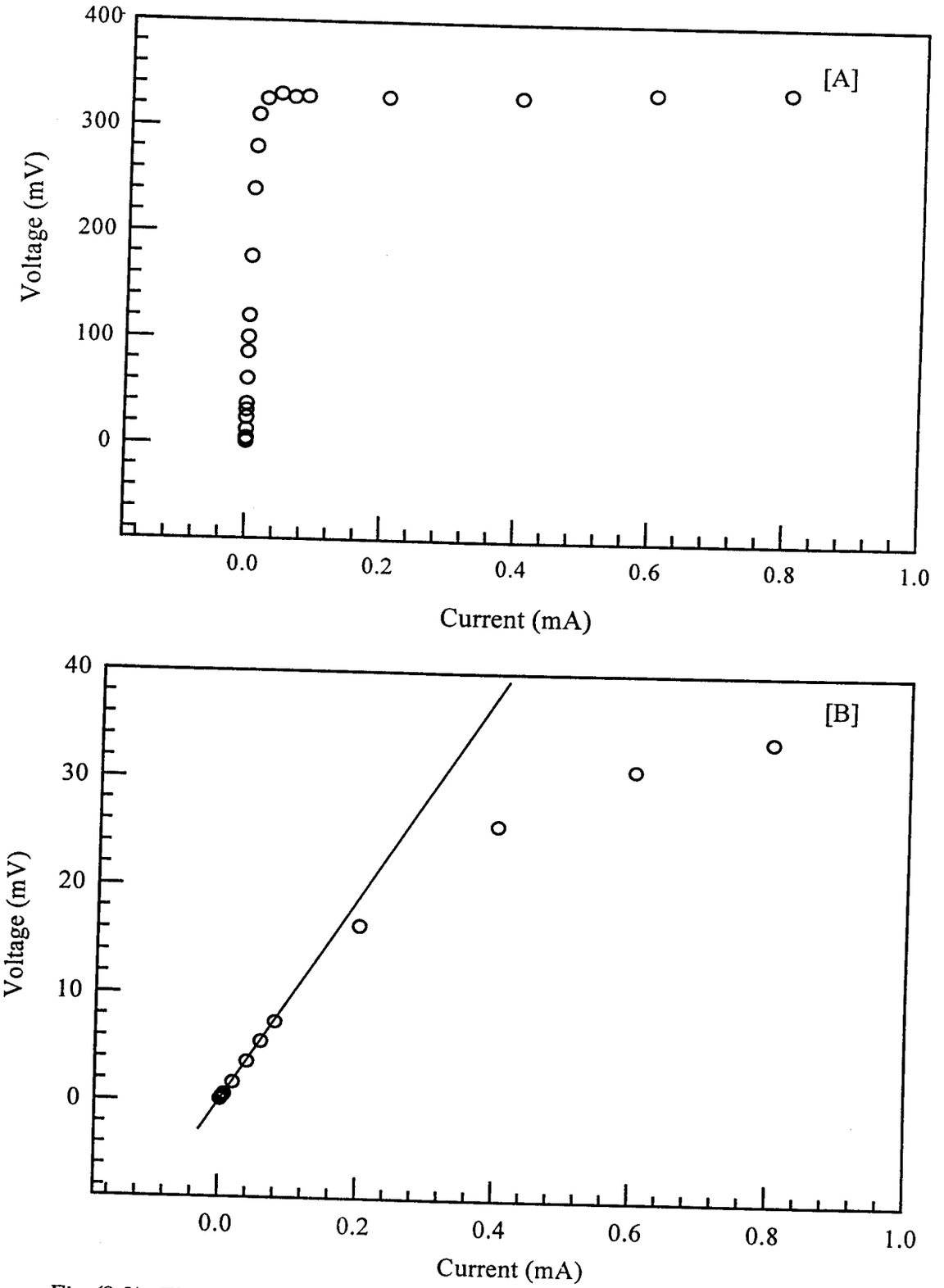

Fig (8.2): The current–voltage characteristics of chemically synthesized Pan at 30 K [A] and 80 K [B].

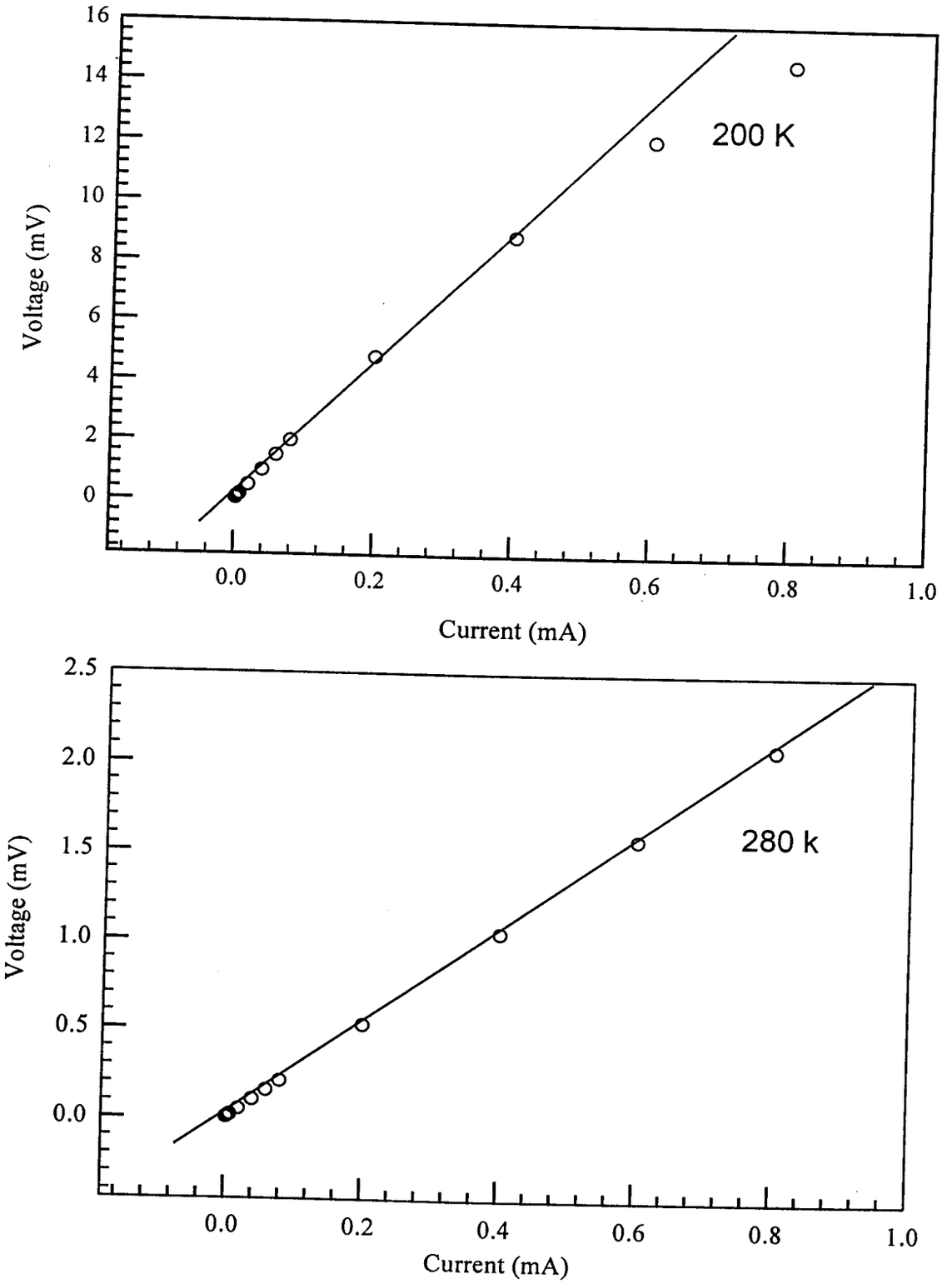

Fig (8.3): The current–voltage characteristics of chemically synthesized Pan at 200 K [C] and 280 K [D].

8.4 Scanning electron microscopy (SEM) images of Pan

SEM images of a Pan film and a pellet are shown in figure 8.4. Different magnifications were used because of the different surface profiles of the film and pellet. Magnifications above (× 1,000) did not provide further significant information for the film. The surface image of the pellets indicates the existence of cracks and inhomoginity in the bulk of the pellet, while the film has a uniform homogenous morphology.

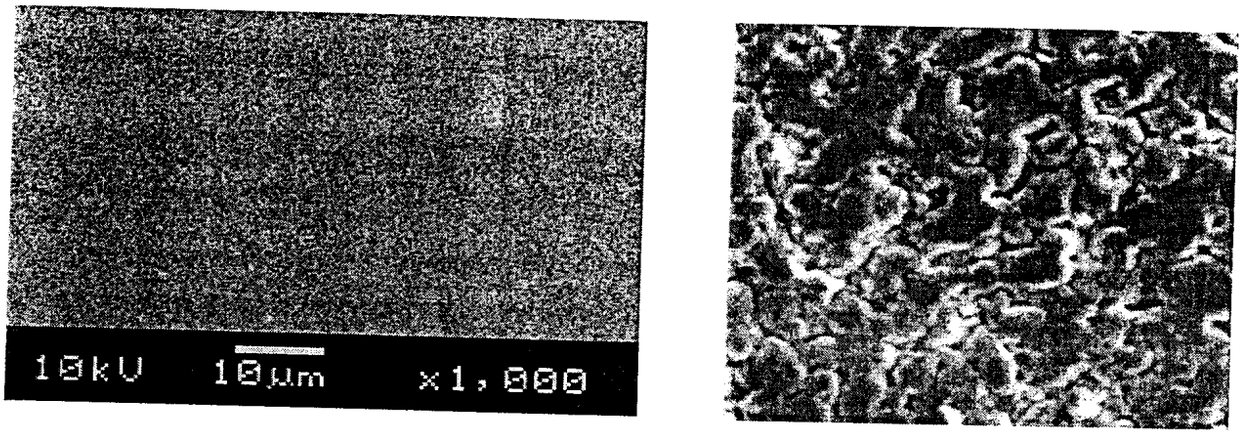

Fig (8.4): The surface images of Pan film (left) and pellet (right) pressed at 7.4 x 10^7 Pa

There is a limitation on conductivity caused by structural defects in the pellet. These results compelled us to measure conductivity at different positions on the pellet surface.

8.5 Positional conductivity for Pan pellets

The four-point probe method was used in obtaining conductivity results for different points on the same pellet, in so as to determine if the conductivity varied with location on the pellet. In this work chemically synthesized Pan was used. Due to the small size of the pellets, only three successive positions (1, 2 and 3) were used as indicated in figure 8.5. Further, table 8.4 outlines the results obtained in the case of two pellets (A and B).

It was observed that the conductivity at different positions on the pellet surface was not always the same. A possible explanation for this positional dependence of the conductivity for the pellet could partly be due to the surface inhomogenity as shown in figure 8.4.

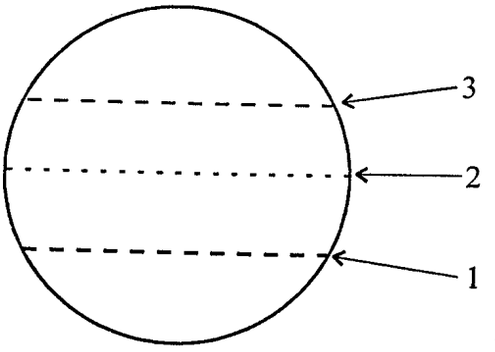

Fig (8.5): The positions on the pellet surface1, 2 and 3.

Table 8.3: Variation of conductivity (σ) on measurement position for Pan pellets (pressed at 47.4 x 10^7 Pa).

Pellet	*Thickness (cm) ± 0.005*	σ_1*(S/cm)*	σ_2*(S/cm)*	σ_3*(S/cm)*
A	0.040	5.58	4.83	6.64
B	0.051	8.43	7.59	8.34

8.6 The effect of pellet pressing pressure on conductivity

Measurements were performed to determine the effect of pressure used in the making of pellets on the conductivity.

The effect of pressure on conductivity can be visualized as denser packing of the material, enabling greater inter-chain contact in fibrilllar CPs. In theoretical terms, the electronic overlap between extended conjugation regions within the chain is partially

extended between chains and between fibers[1]. Pressures ranging from 7.4 x 10^7 to 17.6 x 10^7 Pa were used in pressing pellets. The relationship between conductivity and pressure for Pan in pellet form is shown in figure 8.6.

Within the pressure range used for this study (7.4 – 17.6) x 10^7 Pa there was no indication of a relationship between pressure and conductivity, (3 samples were produced for each pressure reading). However, a study of thin Pan films at pressures up to 22 GPa at room temperature appeared to show enhanced inter-chain charge transport due to sample compression[2].

Figure 8.6, also illustrates that the conductivity of pellets pressed under the same pressure are not necessarily of equal value and there is no clear relationship between pressure and conductivity.

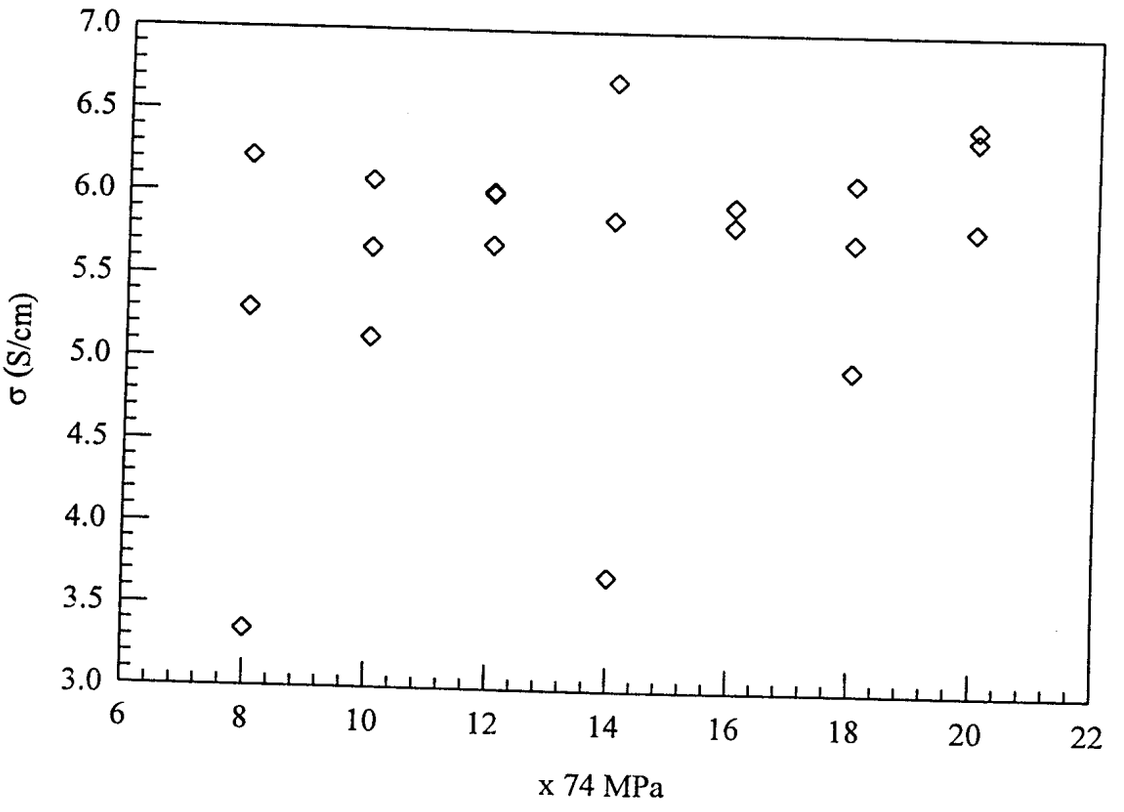

Fig (8.6): The relationship of pellet pressure and conductivity.

8.7 The generalized response of Pan (CSA and HCl doped) in both pellet and film form to annealing

Several factors including, temperature, dopant, moisture content, synthesis conditions and synthesis method differentiate the conductivities of Pan (CSA) and Pan (HCl). One of the aims of this study was to determine if these types of Pan display a generalized behavior under similar conductivity determining conditions. The Pan samples were analyzed at temperatures from 30 to 300 K.

Figure 8.7, illustrates the conductivity-temperature relationship of Pan (CSA) pellet, over the temperature range 30 – 300 K, measured using the Montgomery method. Results indicate; conductivity is responsive to temperature variations above 100K as the graph indicates.

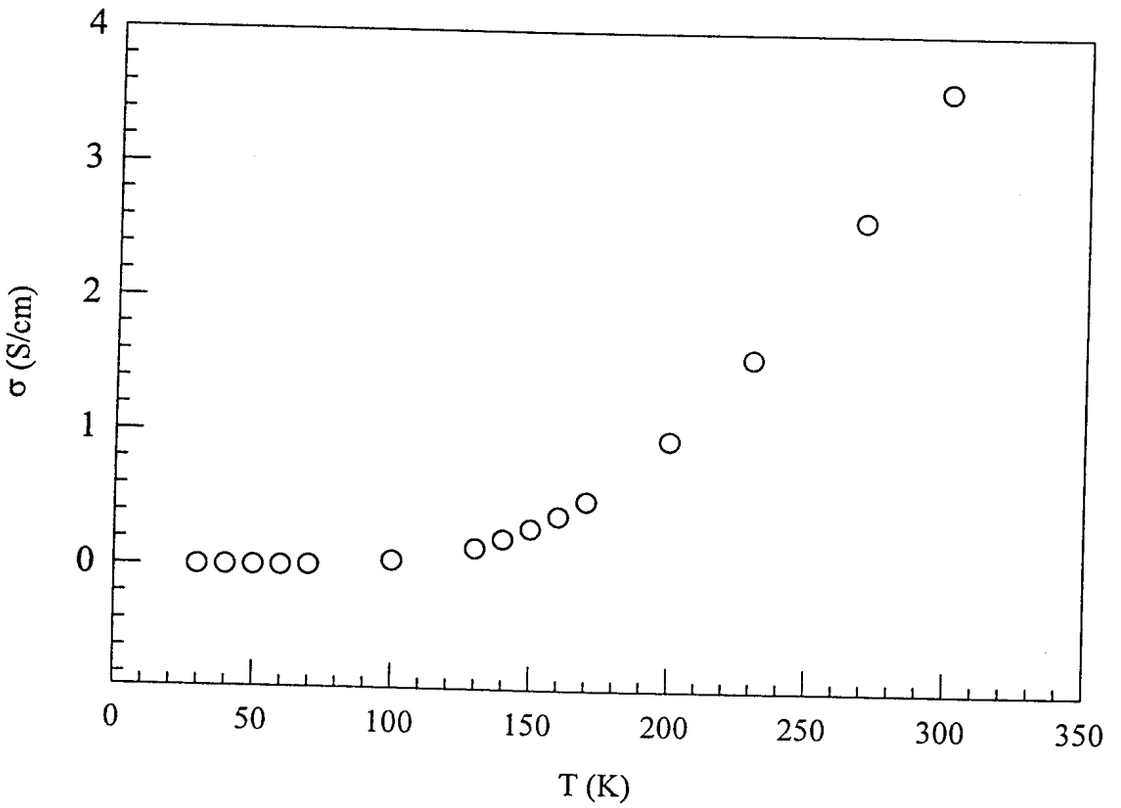

Figure (8.7): Response of Pan (CSA) pellet to temperature variations.

Preliminary experiments, involving annealing a pellet and comparing its current-voltage characteristics before and after annealing (figure 8.8), show an increase in resistance due to the annealing process. The sample was annealed at 373 K for 10 minutes.

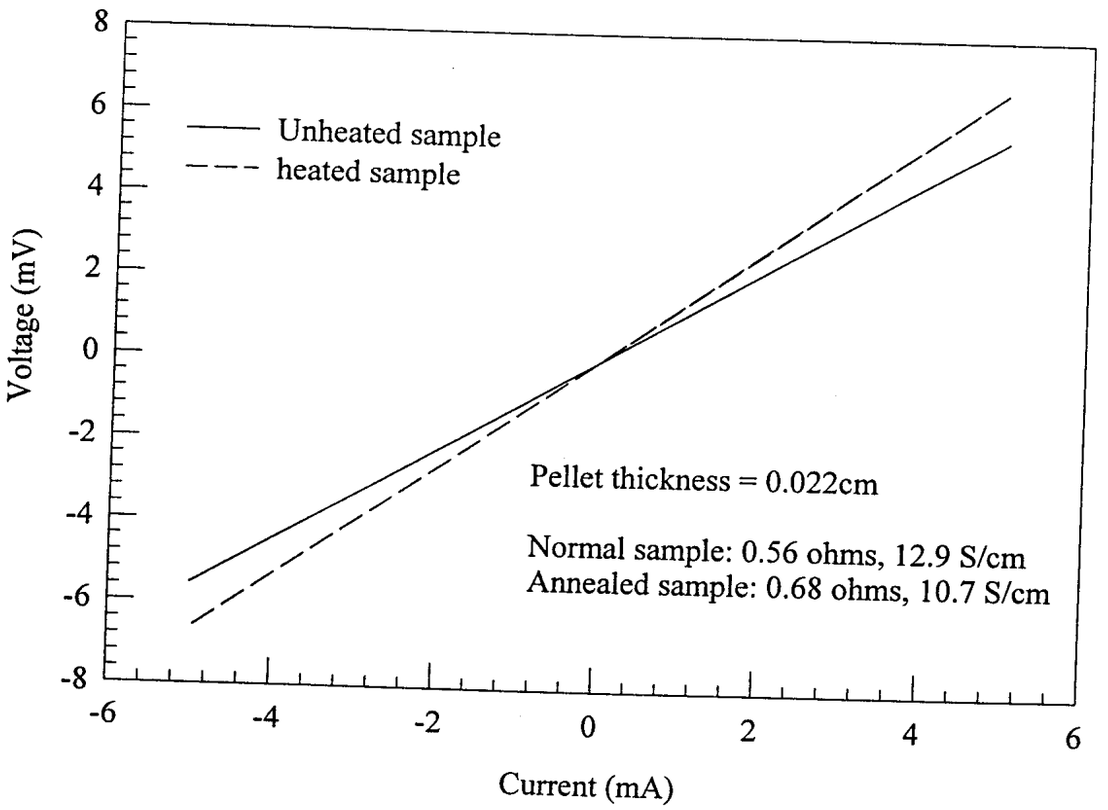

Fig (8.8): Influence of heating on the current-voltage characteristics of a Pan pellet

Further, investigations were done to determine the behavior of the Pan's conductivity as a function of varying temperature. Figure 8.9, illustrates the conductivity-temperature characteristics of Pan (CSA) from 300 to 380 K. The material's conductivity increases with increase in temperature, until approximately 328 K, where after it decreases.

The temperature dependence of conductivity from 300 to 325 K is linear. The decrease in conductivity from 335 to 380 K shows linear temperature dependence and is typical of metals. It would appear that the point $\delta\sigma/\delta T \cong 0$ is a semiconductor/metal transition

region. The point at which $\delta\sigma/\delta T \cong 0$ depends on a number of factors. The following section illustrates that sample annealing rate has a substantial contribution.

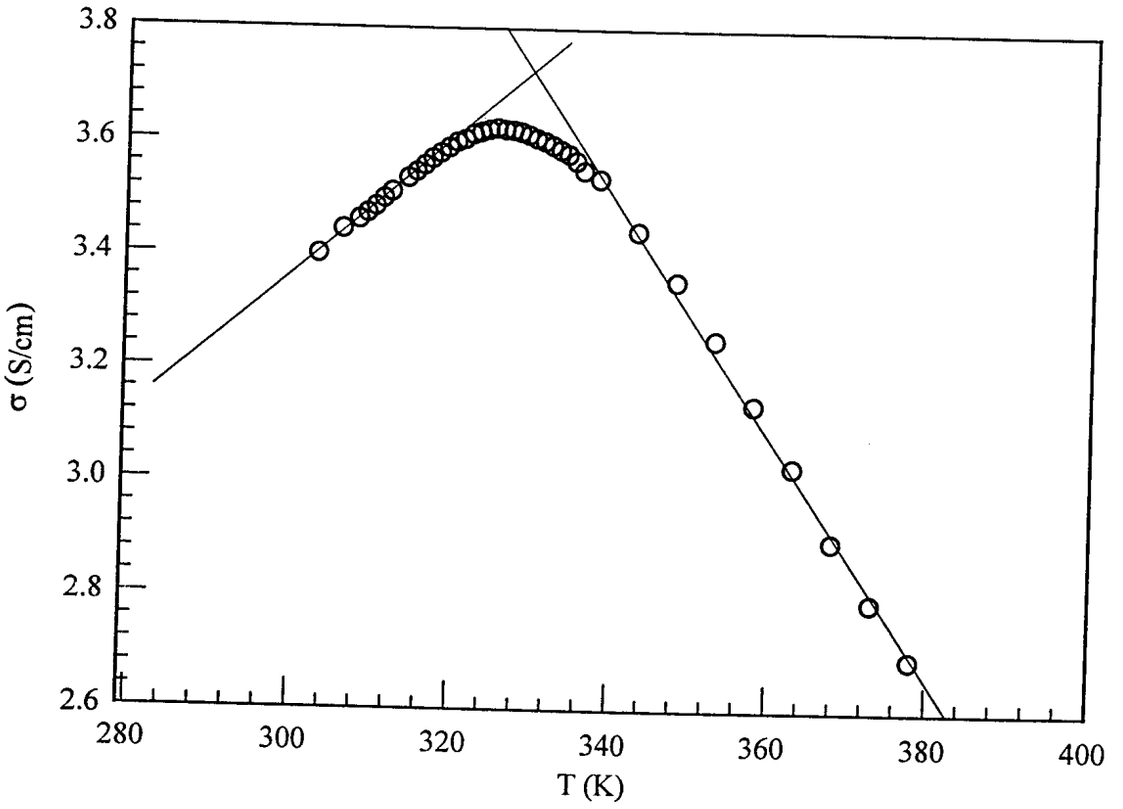

Fig (8.9): The temperature dependence of the conductivity of Pan material.

Thermal analysis shall be used in evaluating the conductivity-temperature relationship. This will be done in order to relate the change in conductivity to the mass loss of the polymer and other possibilities of polymer thermal degradation due to annealing processes.

8.7.1 Response of Pan (CSA) and Pan (HCl) doped to annealing temperature

The reproducibility of the electrical properties of Pan samples is illustrated in the case for Pan pellet and film samples. The conductivity-temperature characteristics of Pan in film

and pellet forms were analyzed and the results are shown in figure 8.10. It was concluded that the form of the Pan has no effect on the general conductivity-temperature response of the material, figure 8.11, both plots show conductivity reaches a point $\delta\sigma/\delta T \cong 0$.

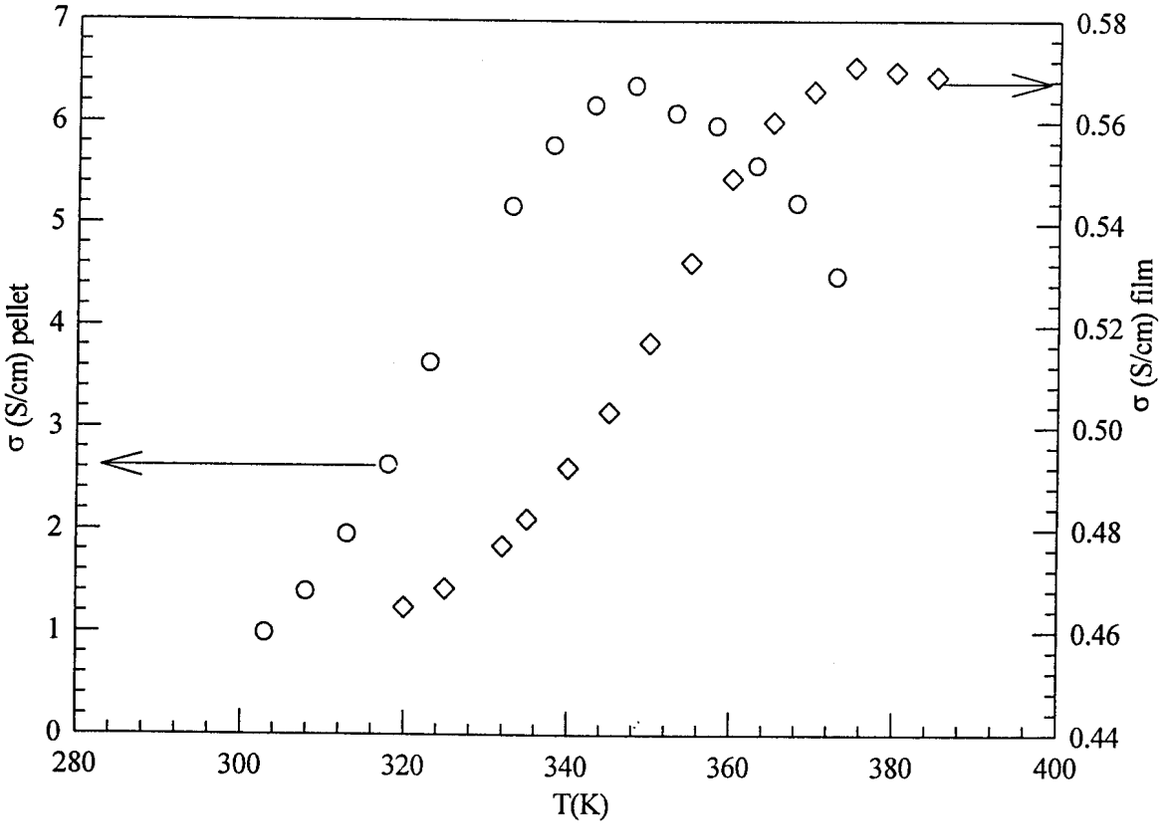

Fig (8.10): Pan (CSA) (o) pellet and Pan (HCl) film (◇) both measured using the Montgomery method.

No difference in behavior was observed for materials with different morphologies, forms and dopant types. **This suggests that transport predominantly involves monomer units and occurs independent of structure.**

8.7.2 The effect of annealing *rate* on Pan conductivity

The four-point probe method was applied for tracing the conductivity response of Pan pellets to annealing and annealing rate. It was found that the $\delta\sigma/\delta T \cong 0$ point depends on the annealing rate. The conduction mechanisms underlying the conductivity profile of figure 8.11 are analyzed in terms of conduction models.

Table 8.5 gives an **estimate** of the temperature readings at which $\delta\sigma/\delta T \cong 0$, for particular annealing rates, as derived from figure 8.11. The point $\delta\sigma/\delta T \cong 0$ shifts slightly to higher temperatures as annealing rate increases. Implying $\delta\sigma/\delta T \cong 0$, results from a heat energy activated process.

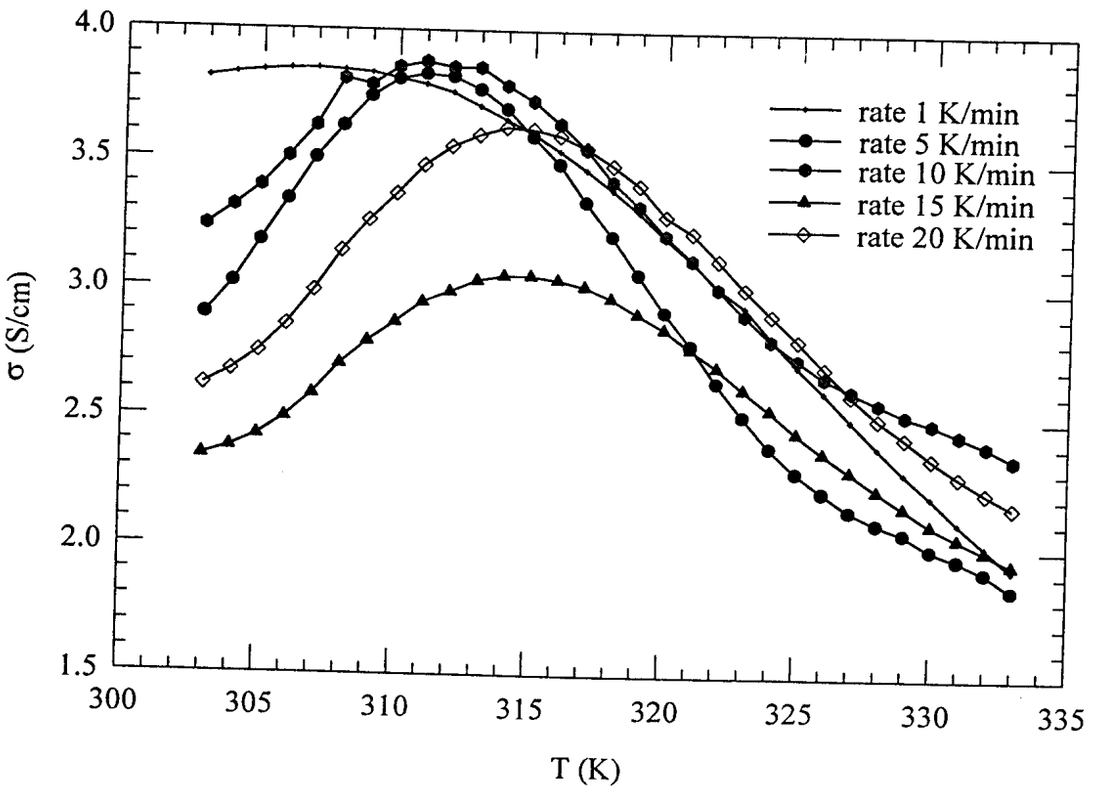

Fig (8.11): The change in conductivity with temperature for different annealing rates. Chemically synthesized Pan pellets were used to obtain these results.

Table 8.5: The relationship of annealing rate to the position $\delta\sigma/\delta T \cong 0$

Annealing rate (K/min)	Temperature at $\delta\sigma/\delta T \cong 0$
1	306
5	311
10	314
15	315
20	316

8.7.3 The conduction models for temperatures above 300 K

The work reported in the previous sections has shown that, the general conductivity response of Pan is similar regardless of the type of Pan and the form of the sample. Pan (CSA) and annealed at 1K/min was used to investigate the fitting of the variable range hopping and the activation energy models at temperatures above 300 K. These results together with thermal analysis and Fourier transform infrared (FTRI) results will help in explaining the conductivity-temperature profiles indicated in figure 8.12.

Figure 8.12 [A], represents Mott's VRH conduction of charge in three dimensions[2] between conducting islands (a plot of $\ln\sigma$ vs. $T^{-0.25}$). VRH model is obeyed for $T < 320$ K for the particular sample. The activated energy model ($\ln\sigma$ vs $T^{-0.5}$), figure 8.12 [B] is obeyed by this particular sample for $T < 319$ K. From the results we cannot state with absolute confidence whether conductivity is governed by VRH in three dimensions.

The thermally activated conductivity is attributed to electron hopping, but the origin and size of the electron localization centers and barriers have not yet been identified[3].

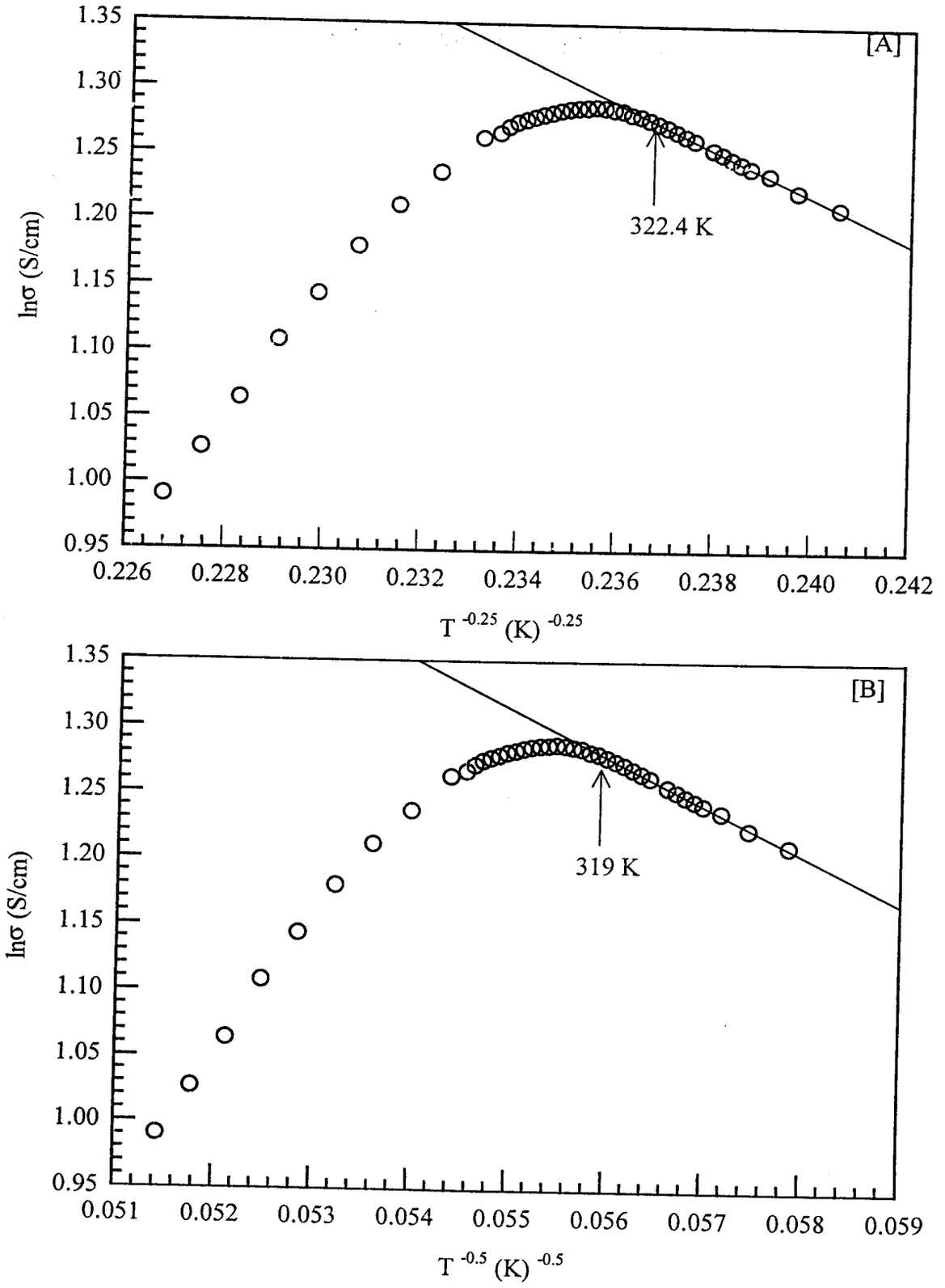

Fig (8.12): 3-D VRH model [A] and activation energy model [B] for Pan (CSA).

8.8 FTIR analysis

Fourier transform infrared spectroscopy was applied in analyzing the effect of annealing on the molecular structure of the polymer. The major objective was to deduce the relationship between conductivity-molecular structure changes as a result of annealing the polymer.

The observed change in conductivity with annealing could be a result of the loss in dopant ions from the polymer. In the event of a dedoping reaction, the spectra of the doped form is expected to change to that of the undoped form. Figure 8.13, shows a comparison of the spectra of the annealed forms of Pan (HC doped). From this figure and the experimentally obtained spectral values of undoped and doped Pan, table 8.6 was constructed. The measuring spectrometer used in this work had a resolution of 2 wavenumbers.

Assuming a dedoping reaction, the wavenumbers 1480 and 1563 cm^{-1} (representing the quinoid ring structure) are expected to move to higher wavenumbers by 17 and 33 values respectively. Tables 8.6 show an average movement of 10 and 18 cm^{-1} for the 1480 and 1563 cm^{-1} wavenumbers respectively, upon annealing. The changes in wavenumbers show a transition of the doped towards the undoped form. However, Pan (HCl doped) will not completely go to its undoped form with annealing as shown by annealing the Pan samples for 73 hrs at 373 K, table 8.6. Accompanying the wavenumber shift is a change in peak intensities, figure 8.13, indicating polymer degradation due to heat energy.

Upon heating the polymer with high intensity laser light, the Raman spectra of figure 8.14 shows that the spectra of doped Pan approaches that of carbon as expected of all polymers. Conclusively, the annealing process results in a slight transition of Pan from the doped to undoped form, loss of chloride ions and polymer degradation.

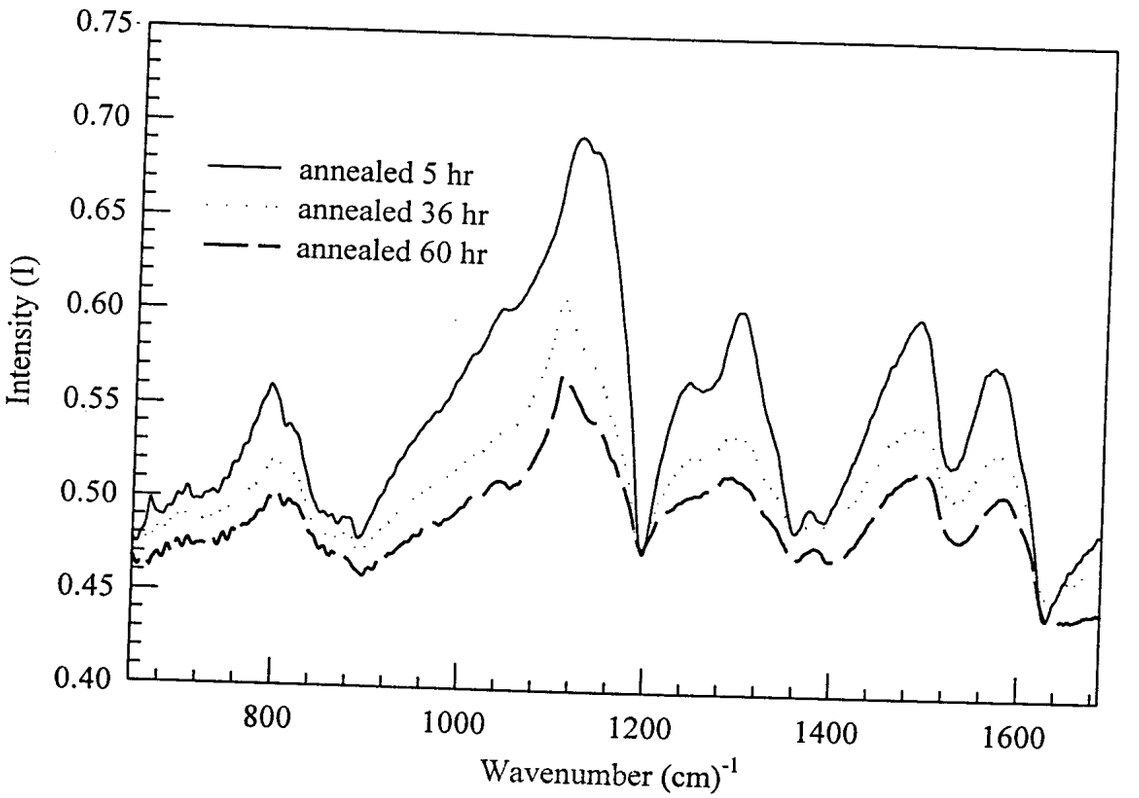

Figure (8.13): The spectral patterns of Pan (HCl doped) samples annealed at 100°C.

Table 8.6: Comparison of the peak positions for Pan samples

HCl doped	795	1106	1294	1480	1563
Annealed 5 hr	794	1119	1294	1490	1577
Annealed 36 hr	800	1103	1290	1490	1584
Annealed 48 hr	797	1103	1290	1490	1581
Annealed 60 hr	806	1103	1277	1494	1584
Annealed 73 hr	813	1110	1274	1490	1581
EB (undoped)	829	1165	1306	1497	1590

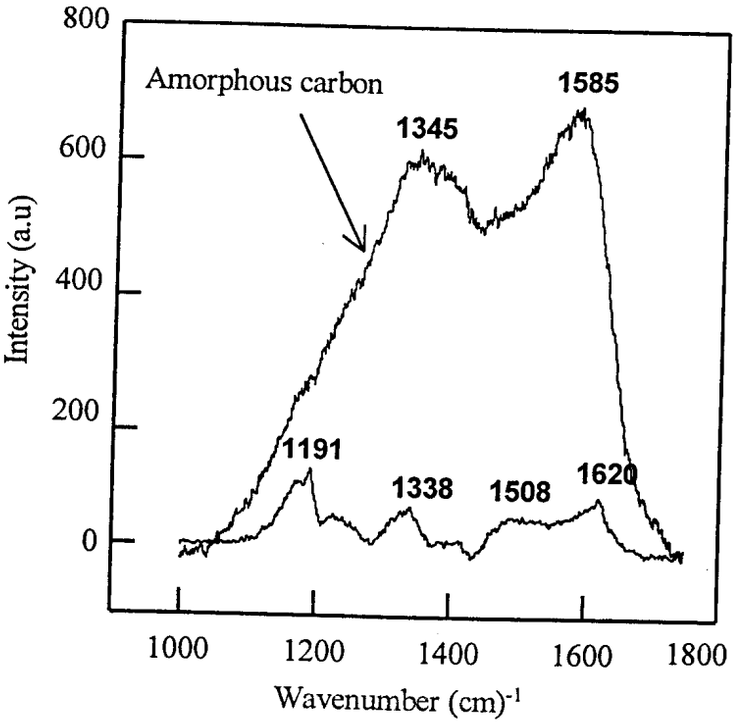

Fig (8.14): The Raman spectra of Pan (CSA) pellet compared to that of amorphous carbon.

8.9 Thermal analysis

Thermogravimetry was used to investigate the loss of moisture from the polymer as a result of annealing and to relate this result to the conductivity response discussed earlier in this chapter. The thermogravimetric (TG) curve, figure 8.15 shows a weight loss in the temperature region 25 – 100 °C, which is due to the loss of water. In this temperature range (figure 8.8-10) the conductivity of the Pan decreases. The second mass loss starting at about 250 °C is attributed to thermal degradation of the polymer.

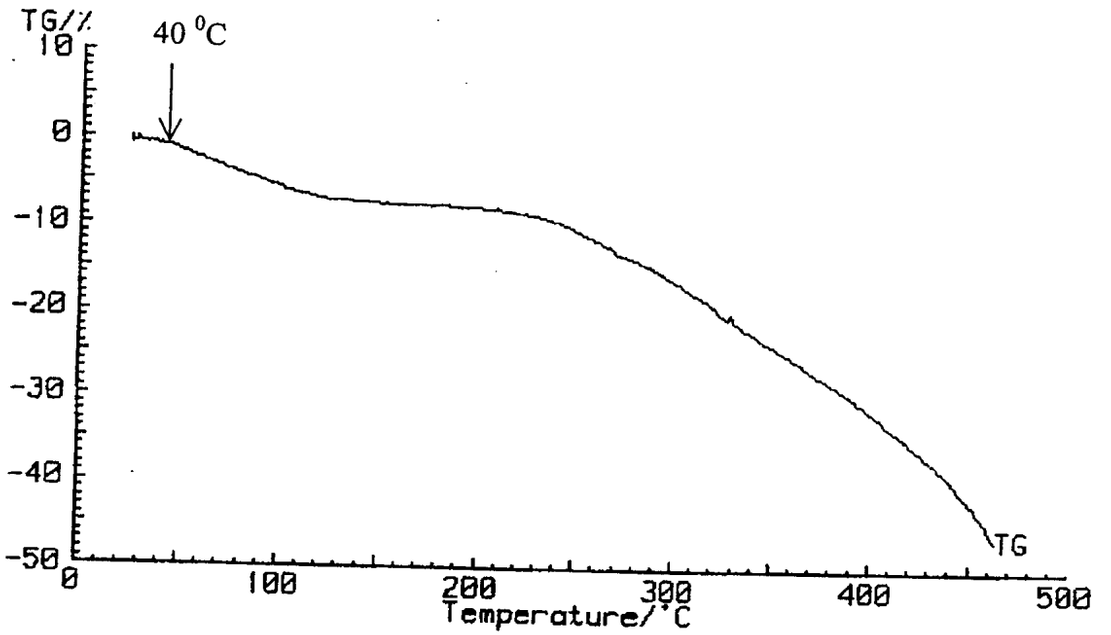

Fig (8.15): TG graph shows the loss of mainly water around 100 °C.

8.10 Conductivity in the temperature range 30 < T (K) < 300

Conductivity in the temperature range 30 < T (K) < 300, has been useful in determining the dimensionality of conduction in the polymer, conduction model of best fit and whether conduction in this temperature range is semiconducting, insulating or metallic.

Conductivity of the materials is analyzed in terms of the conduction models described in chapter 5. Figure 8.16 (for Pan (CSA) pellet sample) shows that resistivity (ρ) of the polymer is stable as temperature goes down from 300 to 100 K and increases from 100 to 30 K, the degree of temperature dependence of resistivity increases substantially at T < 100 K.

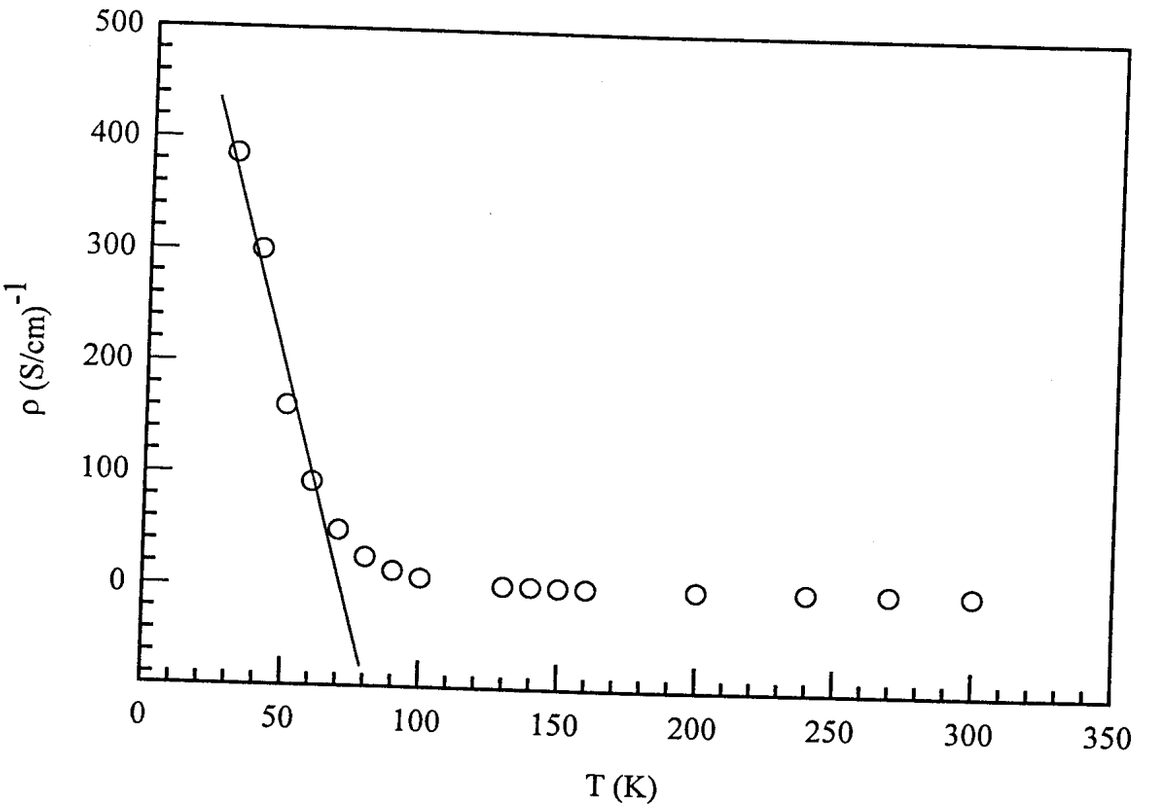

Fig (8.16): Variation of resistivity with temperature for chemically synthesized Pan.

The electrical properties of doped polymers are strongly dependent on the extent of disorder present in the material. The extent of disorder is generally characterized in terms of the temperature dependence of resistivity[2]. The resistivity coefficient of the material $\delta\rho/\delta T$, show little temperature dependence of conductivity for; $\rho_{(315\ K)}/\rho_{(310\ K)} = 1.02$, $\rho_{(320\ K)}/\rho_{(315\ K)} = 1.02$ and $\rho_{(325\ K)}/\rho_{(320\ K)} = 1.01$. But $\rho_{(300\ K)}/\rho_{(30\ K)} = 823.5$, indicating Pan is insulating at 30 K.

The Kivelson model and the VRH in 3-D were applied in analyzing the conductivity of Pan (CSA) and chemically synthesized Pan. From the previous sections there is not much significant difference between the activated model and VRH model in 2 and 3 D.

8.10.1 The conduction models

Several authors have examined the different conduction models and they have concluded that the VRH model in 3-D represents conduction in Pan satisfactorily. It is presumed however, that the overall conductivity observed, is a superposition of more than one conduction phenomenon.

The linear dependence of the measured variables (($\ln\sigma$ vs. $T^{-0.25}$) for the 3-D VRH model and ($\ln\sigma$ vs. $\ln T$) for the Kivelson model in figures (8.17, 8.18 and 8.19) would indicate an agreement between the conduction model and the conduction phenomenon. For the present section of this current chapter, the agreement between the conduction phenomenon and the conduction models is of prime importance. From these results, we shall deduce the model which best describes conduction in our samples of Pan.

8.10.1.1 Mott's VRH in 3-D

The micrographs of CP pellets and films demonstrate that the polymer solids consist of a heterogeneous structure of fibres and grains[1]. An idealisation of this structure was shown in figure 4.5 chapter 4 section 4.2.2. It is perhaps more accurate to characterize the conduction process in CPs as the hopping of electrons between these charged carriers, a basis for "hopping " models of conduction.

Figures (8.17, 8.18 and 8.19) are the Kivelson and 3-D VRH responses for the following materials; Pan (CSA) pellet, Pan (HCl) and Pan (CSA) film respectively. The Mott's VRH is a phonon assisted quantum-mechanical transport process in which a balance is obtained between the thermodynamic constraint on a charge carrier moving to a nearby localized state of different energy, against the quantum-mechanical restraint of a carrier moving in a localized state of a similar energy, but spatially remote[4]. This process leads to characteristic temperature dependence represented by the Mott's VRH conduction models, although there are other conduction mechanisms, which can, under certain conditions, also give such temperature dependence[4]. From the results we can conclude

that conduction phenomenon for our samples of Pan obeys the 3-D VRH model over the temperature range 30 – 300 K satisfactorily.

8.10.1.2 Kivelson model

This model has been largely used in representing the conductivity of lightly doped Pan samples. In this model, the conductivity follows the power law[3], $\sigma(T) \propto T^n$ where, n > *10.*

Figures ((8.17, 8.18 and 8.19)) are the responses of Pan (CSA) pellet, Pan (HCl) pellet and Pan (CSA) film respectively. Kivelson model is obeyed at T < 260, for all our samples. Estimates of the upper temperature limits for the Kivelson model are inserted in the figures.

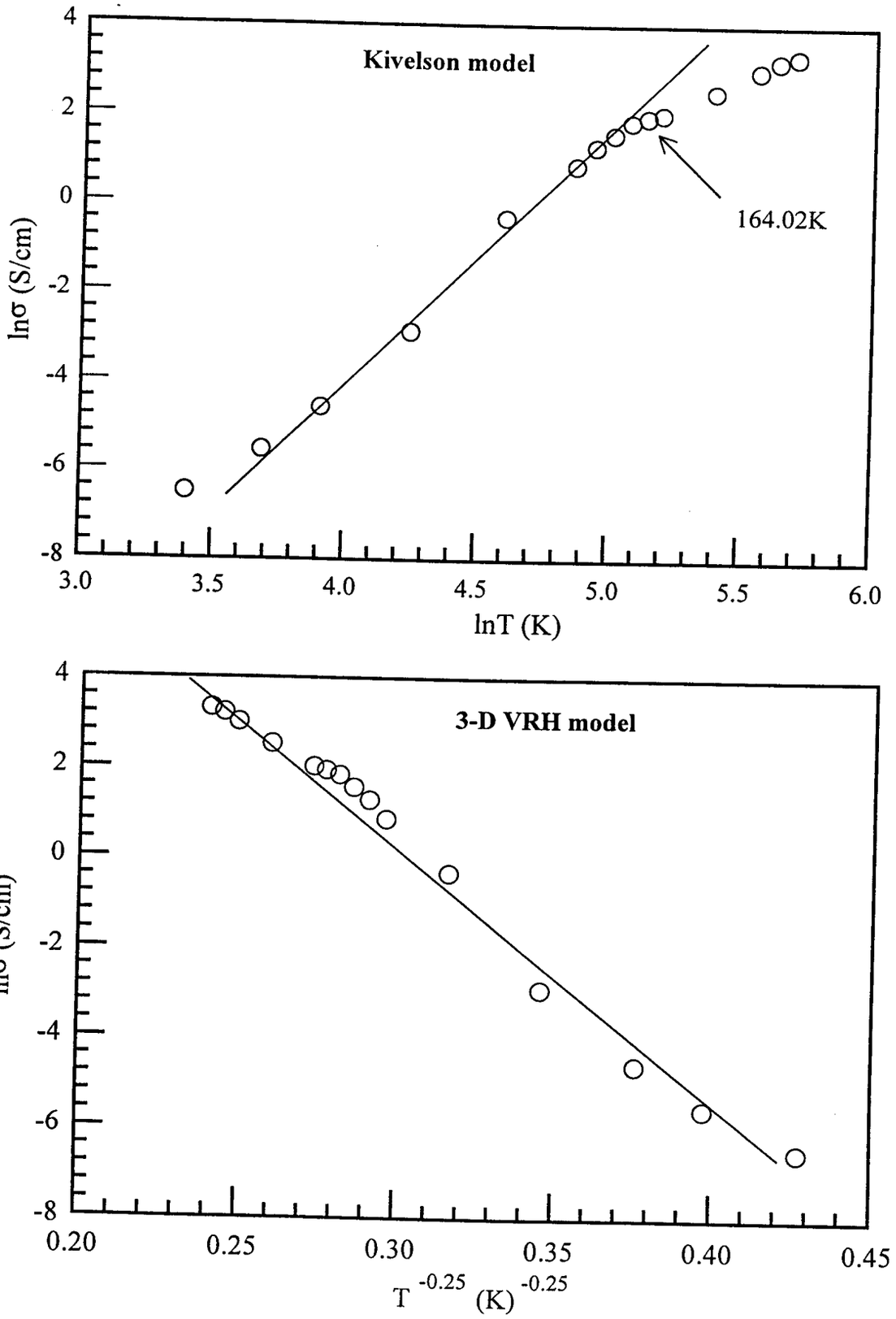

Fig (8.17) The Kivelson and 3–D VRH models for Pan (CSA) pellets.

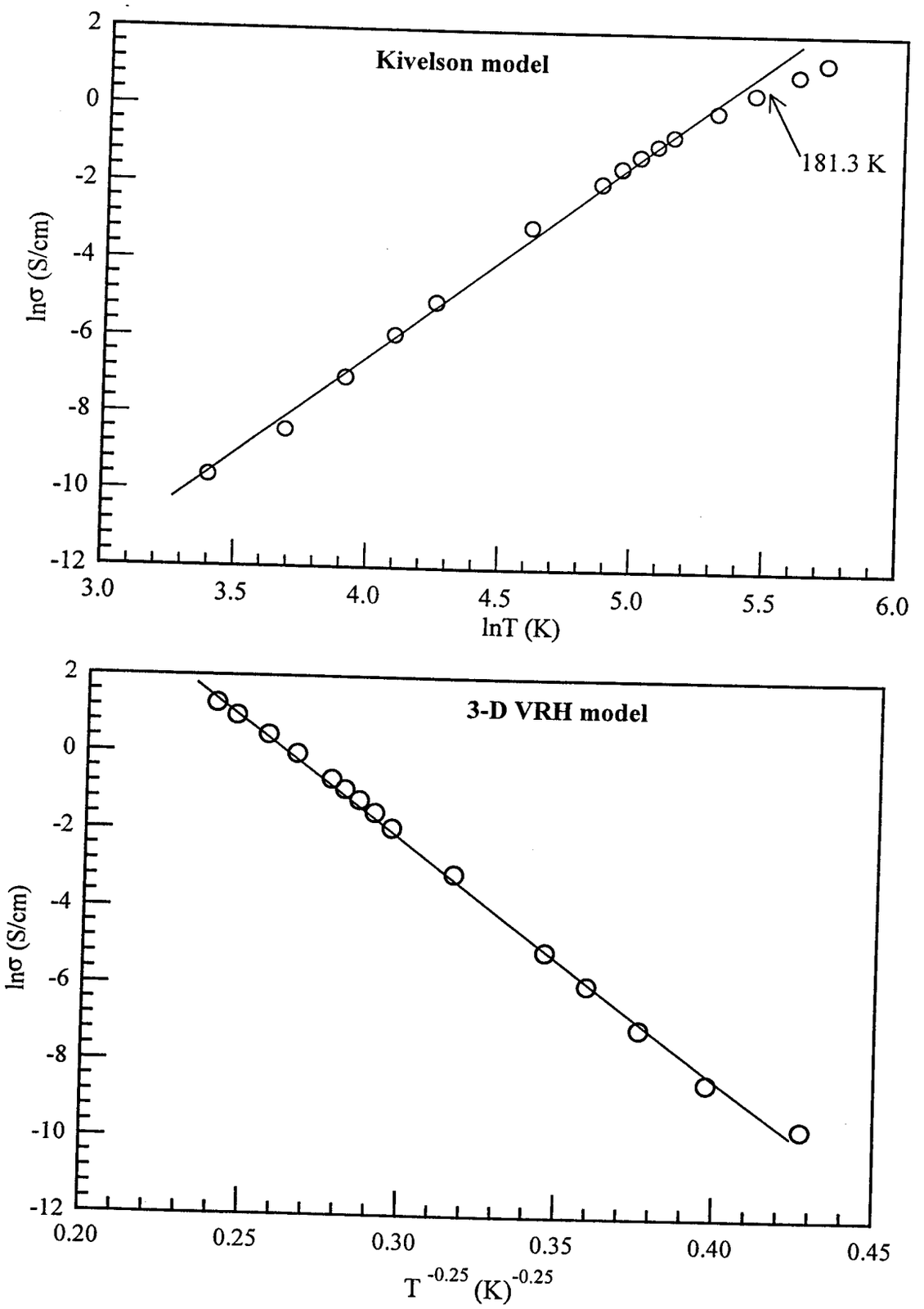

Fig (8.18): Kivelson and 3-D VRH models for Pan (HCl) pellets.

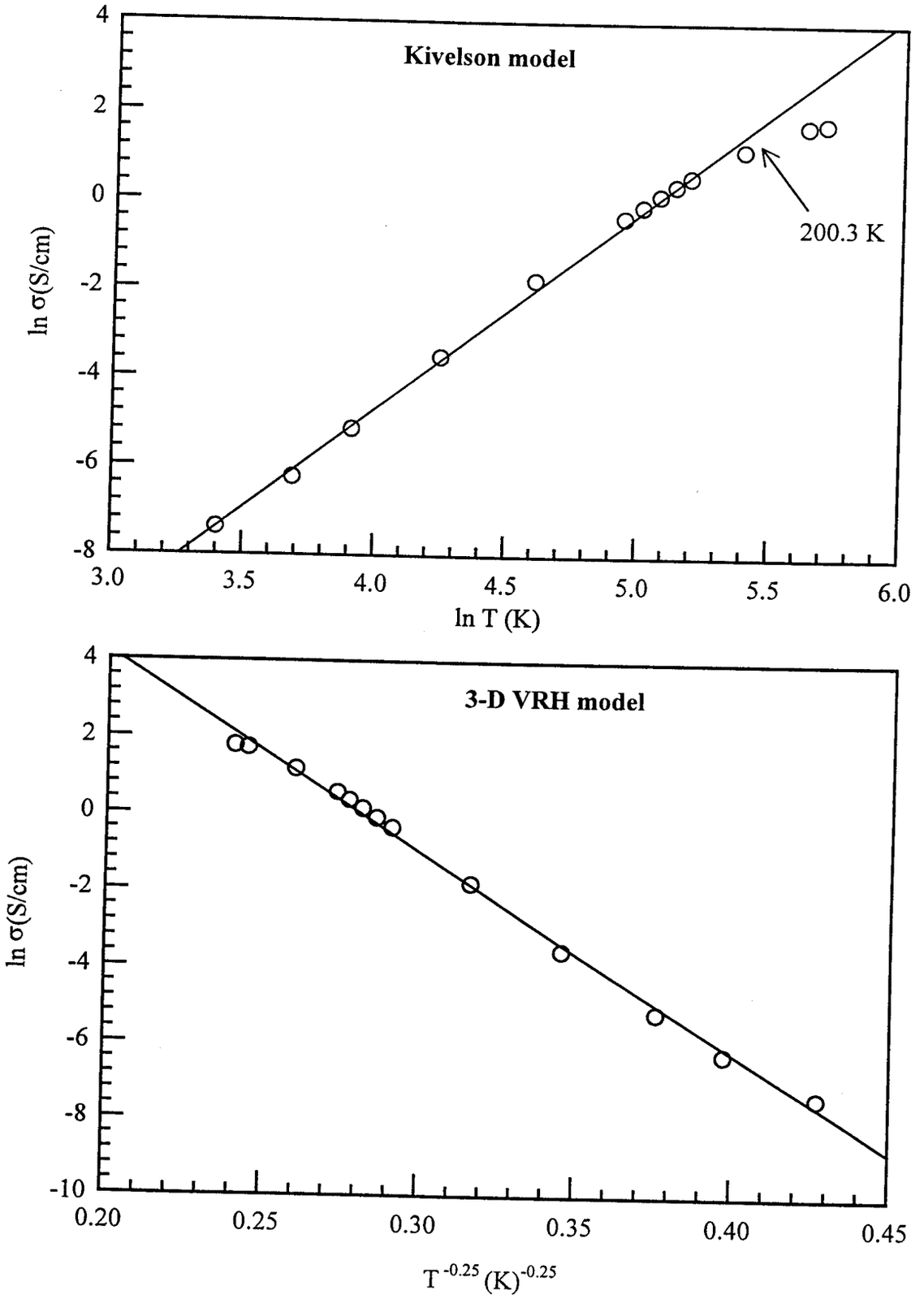

Fig (8.19): Kivelson and 3-D VRH models for Pan (HCl) films.

Reference

1. Conducting Polymers, Fundamentals and Applications, (Ed. P. Chandrasekhar), Kluwer academic publishers, Boston (1999).
2. R. Menon, C. O. Yoo, A. J. Heeger, Phys. Rev. **B 48**, 17685 (1993).
3. M. Gosh, A. Barman, S. Chatterjee, Phys. Lett. A **260**, 138 (1999).
4. D.S. Maddison, T. L. Tansley, J. App. Phys, **72**, 4677 (1992).

Chapter 9

Discussion

i. In stating the conductivity of a sample of Pan, other conductivity determining factors such as sample thickness, temperature, form of the sample and dopant used need to be mentioned.

ii. Specific conductivity values for CPs can not be reproduced even for samples derived from the same source.

iii. Low power dissipation of about 0.1 μWatt gives a more accurate measure of the material's electrical properties.

iv. The positive resistivity coefficient at temperatures below 300 K implies semiconducting behavior.

v. $\sigma(T)$ dependence is extremely weak for Pan materials used in the present work.

vi. Moisture is important for charge transfer.

vii. Conductivity is temperature activated.

viii. Annealed samples show Ohmic behavior.

ix. The fall in conductivity as a result of annealing the sample is attributed to the loss of moisture, degradation of the polymer and loss of the volatile hydrochloric acid.

x. There is a slight shift of the spectra of the doped form towards higher wavelength upon annealing.

xi. 3-D charge transfer sufficiently describes conductivity in Pan at $T < 320$ K.

xii. Application of conduction models to temperatures above 330 K is less accurate, since thermal analysis has shown the loss of water and other gaseous materials from the polymer.

xiii. The strong temperature dependence as temperature is lowered down to 30 K (compared to metals) arises from a combination of mesoscale inhomogeneity ("metallic islands") and microscopic disorder (localization of the electronic wave functions) both of which are indicative of the quality of the material. Thus Pan has

been characterized as a collection of metallic islands separated by insulating barriers[1].

Reference

1. M. Reghu, Y. Cao, A. J. Heeger, Phys. Rev. **B 47**, 1758 (1993).

Chapter 10

Conclusion

i. Thermal analysis has shown that the loss of moisture and other substances from Pan, affects polymer conductivity, a way of replenishing the moisture content of CP devices based on Pan will ensure their accuracy and longer device life span.
ii. The value of the applied current used for Pan materials has an effect on the current-voltage characteristics.
iii. The conductivity-temperature characteristics of all types of Pan are the same, (commercial Aldrich CSA and HCl doped, electrochemically synthesized and chemically synthesized.
iv. Conductivity values of Pan are not reproducible whether Pan is in pellet or film form.
v. Pan shows semiconducting behavior for $30 \leq T\ (K) \leq 300$.
vi. The VRH in 3 or 2 dimensions equally represented the conductivity in Pan.
vii. For hopping transport, conductivity increases with temperature in contrast to the decrease in conductivity with temperature for band conduction.
viii. The ratio σ (30 K)/ σ (300 K) for Pan at 30 K is indicative of insulating behavior.

Amongst other factors we could not study was the effect of vacuum on conductivity. It is assumed the process of pumping vacuum, in the cryostat, for low temperature measurements, results in dehumiditizing Pan and thus affects its conductivity.

Conductivity should be mainly due to hopping process that is hopping between localized electronic states, which are distributed at random in space and energy. The data do not really allow it to be possible to distinguish between two and three-dimensional conductivity.

Since there is a finite density of states at the Fermi energy (as inferred from the temperature-independent Pauli susceptibility) the increase in resistivity at low temperatures results from disorder-induced localization[1].

10.1 Motivation for future work

One of the major problems encountered with polyaniline was the varying of conductivity even for samples derived from the same powder source. This would imply one cannot state the conductivity value of polyaniline with absolute certainty. The study of the distribution of chain lengths in polyaniline should be undertaken together with a study to synthesis a polymer of uniform chain length.

The study of conducting polymers offers many opportunities. Even though charge transfer characteristics of conducting polymers are still not fully understood, the reproducibility of electronic, optical and photoelectrical properties to mention a few has allowed it possible to design and fabricate conducting polymer based devices. It is proposed that the next stage of this study should include a study towards coming up with devices that would have several advantages over the conventional material made devices. Devices of particular importance would be the study on polymer-based solar cells and polymer light emitting devices.

Several other conducting polymers including those mentioned in chapter 2, could be studied in place of polyaniline.

Reference

1. R. Menon, C. O. Yoo, A. J. Heeger, Phys. Rev. **B 48**, 17685 (1993).